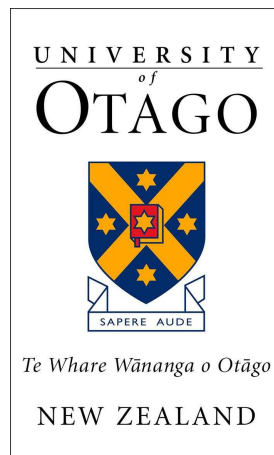# Self-induced temperature gradients in Brownian dynamics

Jack Devine

The University of Otago

A THESIS SUBMITTED FOR THE PARTIAL FULFILLMENT OF BACHELOR OF SCIENCE WITH HONOURS IN PHYSICS AT THE UNIVERSITY OF OTAGO, DUNEDIN, NEW ZEALAND

Supervised by
Dr M. W. Jack

September 23, 2016

Abstract

As Brownian particles diffuse over a potential landscape, they draw energy from their environment in the form of heat, causing temperature gradients. We define a self-consistent set of non linear partial differential equations to describe these self-induced temperature gradients. We obtain theoretical steady state solutions to the equations of motion and employ numerical techniques to explore the dynamical properties of the system. We find the Kramers' rate for our modified view of Brownian dynamics and we make concrete observations of Brownian cooling and the reverse Landauer blowtorch effect. We show that these phenomena can significantly alter the dynamical behavior of a particle on a tilted periodic potential. In particular, we show that for certain parameters, the motion of the particle can be retarded significantly. This has direct consequences to biology in the context of molecular motors as well as the dynamics of colloidal particles.

Acknowledgments

First I would like to Acknowledge my supervisor Dr. Michael Jack for helping me through this difficult project and always being available to give me advice. As well as this, I would like to acknowledge Professor Michael Colombo, Vaughan Weatheral, Luke Trainor and Loren Kersey for reading very early drafts of this report, they helped me to remove many mistakes. Finally, I would like to thank my colleagues in the honors room for their camaraderie and banter throughout the year.

At the atomic level, we have new kinds of forces and new kinds of possibilities, new kinds of effects. The problems of manufacture and reproduction of materials will be quite different. I am, as I said, inspired by the biological phenomena in which chemical forces are used in a repetitious fashion to produce all kinds of weird effects (one of which is the author).

Richard Feynman
– There's Plenty of room at the bottom (1959).

Contents

Chapter 1

Introduction

To mention all the mineral substances in which I have found these molecules, would be tedious; and I shall confine myself in this summary to an enumeration of a few of the most remarkable. These were both of aqueous and igneous origin, as travertine, stalactites, lava, obsidian, pumice, volcanic ashes, and meteorites from various localities. Of metals I may mention manganese, nickel, plumhago, bismuth, antimony, and arsenic. In a word, in every mineral which I could reduce to a powder, sufficiently fine to be temporarily suspended in water, I found these molecules more or less copiously; and in some cases, more particularly in siliceous crystals, the whole body submitted to examination appeared to be composed of them.

Robert Brown, on what we now call Brownian particles.

1.1 Brownian motion

Brownian motion is the motion that occurs when looking at microscopic particles that are suspended in a fluid, Brownian motion is highly random and is due to molecules in the fluid colliding with the Brownian particle trillions of times per second. Brownian motion occurs on the micro meter to nano meter scale [1, 2]. Particles of this size are constantly bombarded by the environment causing some people to use the term "molecular hurricane" [3].

Brownian motion was first observed by Robert Brown in 1827 [4]. In these observations, Brown saw that microscopic particles (for example pollen grains) were in constant motion. He noticed that this motion was still present in inorganic material including granite and ground up sphinx bones. Over half a century later, Einstein posited that Brownian motion was due to constant bombardment by water molecules in the surrounding environment [5]. Einstein's theory of Brownian motion was then experimentally verified by Perrin [6].

In principle if one knew the momenta and positions of all of the Brownian particles and the molecules in the fluid, then one could use Newtonian mechanics to fully predict the future state of the system. In this project, we will be looking at systems with particle number on the order of Avagadro's number ($N \sim 10^{23}$). With systems of this size, a Newtonian description is completely impractical, so instead
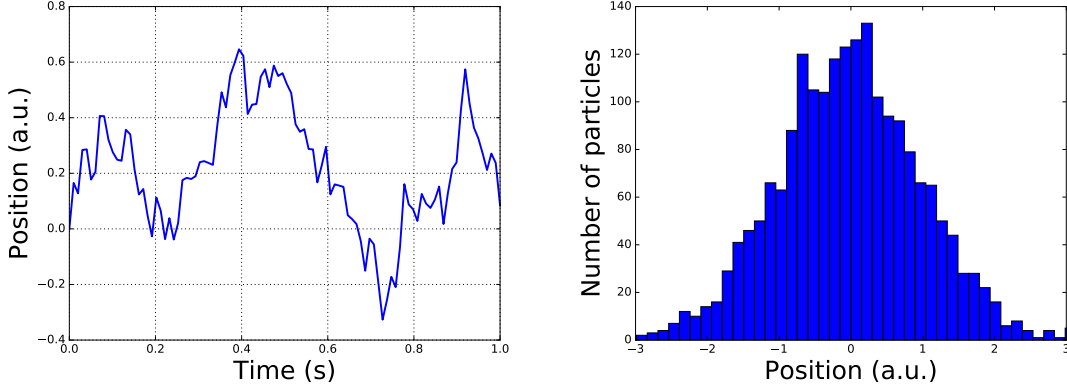
Figure 1.1: Cartoon demonstration of Brownian motion. (a) Trajectory of a single tagged Brownian particle. The particle is being forced around randomly by the molecular hurricane. Since there is no net force on the particle, we find that the particle makes no net progress over time. (b) An ensemble of Brownian particles simulated for 1 second, here we see that the mean displacement is zero because there is no background force on the particles, this statistical nature of the particles motivates us to view the particles in a probabilistic sense.

we will use a statistical approach. In this view the motion of a single Brownian particle suspended in a fluid at a given temperature (which we will call the bath) is stochastic.

Brownian particles can be described stochastically by the Langevin equation which is essentially Newton's second law with the addition of a random force applied to it, we can write this as:

$$m\ddot{x}(t) = -\gamma\dot{x}(t) + F[x(t)] + \xi(t),\tag{1.1}$$

where γ is the viscous friction coefficient of the Brownian particle, $F[x(t)]$ is an external force on the particle and $\xi(t)$ is Gaussian white noise with zero mean and has auto-correlation given by $\langle\xi(t)\xi(s)\rangle = 2\gamma k_B T\delta(t-s)$ where k_B is the Boltzmann constant and T is the temperature. $\xi(t)$ is the thermal noise of the environment, this is the force produced by the collisions of the Brownian particle with particles in the environment.

The regime of Brownian motion that we will discuss is the so called over-damped limit, in this regime the mass of the particle is so small that we ignore the inertia of the particle. Therefore, all of the energy of the system is quantified by the potential energy of the particle and the thermal energy of the bath [7–10]. The over-damped regime of a Brownian particle can be described stochastically by the Langevin equation

$$\gamma\dot{x}(t) = F[x(t)] + \xi(t).\tag{1.2}$$

Figure 1.1 illustrates this motion for the case when $F[x(t)] = 0$. We can also describe Brownian motion by following the evolution of the probability distribution of a single Brownian particle which we will write as $P(x, t)$.

The probabilistic view of Brownian motion on a potential is illustrated in Figure 1.2. In Figure 1.2, we do not have any knowledge of the individual particles in the
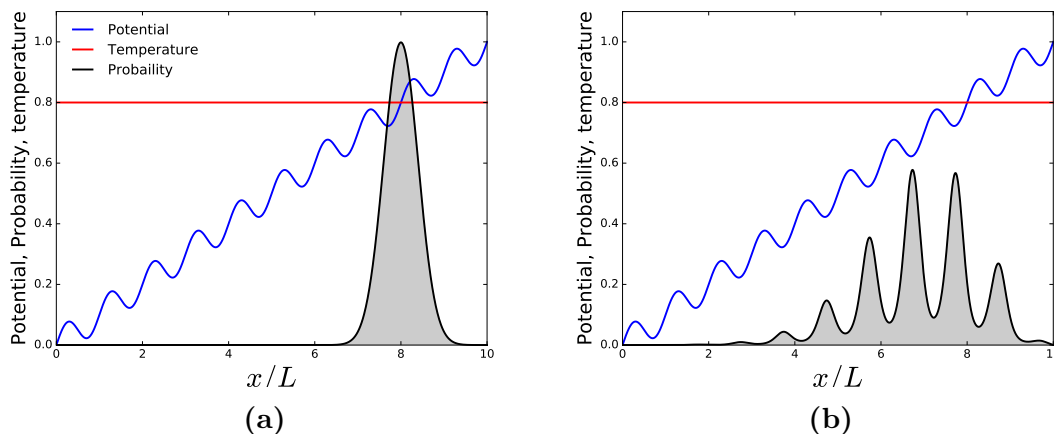
Figure 1.2: Schematic showing the probability density of particles diffusing in a one dimensional tilted periodic potential at a fixed temperature.
(a) Initial probability distribution, (b) is the state of the system after 2.0 dimensionless time units. We see that the particles tend to drift down the potential as they diffuse. This drift will be called the current J which we will quantify in § 2.1. In § 2.4, we will define the dimensionless time and length scale used in the calculations for this figure.

ensemble, instead, we only know about the probability distribution that describes them. The situation in Figure 1.2 is described by the Smoluchowski equation [11]. In this report we will use the Smoluchowski equation to model a Brownian particle, although it is useful to keep in mind that the underlying dynamics are stochastic. The Smoluchowski equation can be written as

$$\frac{\partial P(x,t)}{\partial t} = \gamma^{-1}\frac{\partial}{\partial x}\left(P(x,t)\frac{\partial V(x,t)}{\partial x} + k_B T(x,t)\frac{\partial P(x,t)}{\partial x}\right), \qquad (1.3)$$

where $P(x,t)$ is the probability density of finding the particle is at x at time t, $V(x,t)$ is the potential which from now on we will take as being time-independent and $T(x,t)$ is the temperature of the environment. The force on the particle is given by $F(x,t) = -\frac{\partial V(x,t)}{\partial t}$ with this in mind, equation 1.3 describes the same physical situation as equation 1.2. Intuitively, the first term of the equation represents the force that the potential applies on the particle and the second term represents the diffusion of the particle due to thermal noise.

1.2 Brownian motors

Brownian motors are devices that can use stored chemical energy to create directed motion on a microscopic scale and are ubiquitous in biology where, by transforming energy from one degree of freedom to another, they are used to perform important tasks in cells [12–14]. Recently, thanks to improvements in imaging techniques, researchers have been able to make highly detailed images of these motors and their working components [15]. As well as being able to crank a rotor in the
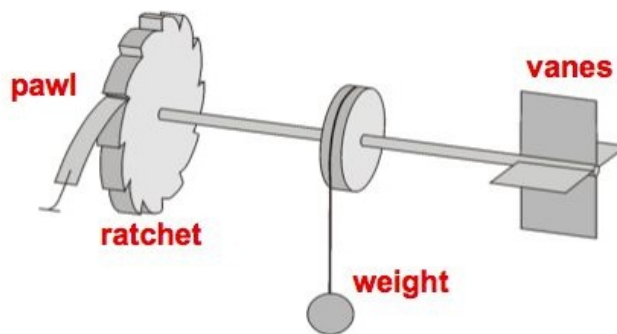
Figure 1.3: The Feynmann ratchet and pawl [24]. The ratchet is located in a bath at temperature T_1 and the vanes are in a bath at temperature T_2. (Figure taken from http://pof.tnw.utwente.nl/research/granular/ratchet)

in the fashion of a traditional motor, Brownian motors are also able to pump ions against a gradient and translocate molecules [2, 13, 16, 17].

Artificial Brownian motors have also been investigated in the laboratory. For example Ref [18] created a stochastic heat engine by placing a single colloidal particle in a time dependent optical trap. Likewise, Ref [19] placed a colloidal particle in an optical tweezer and drove the particle with explosive vaporization of the surrounding liquid, thus demonstrating a thermal mechanism for Brownian motors. Ref [20] placed DNA molecules in a time dependent potential to transport the molecules. Brownian ratchets capable of walking along a track have been implemented in the laboratory recently [21–23]. In order to improve on these designs and to approach the efficiency present in nature, we will have to understand the physics of Brownian dynamics very clearly.

The term Brownian motor is not a misnomer, a Brownian motor can be modeled as a Brownian particle diffusing over a potential [2]. In the case of Brownian motion it is natural to think of the particle moving in a spatial coordinate x, however in the case of Brownian motors the interpretation of the coordinate x is more abstract. In general x will be a degree of freedom for the system, examples include reaction coordinates for a chemical reactions, or in the case of rotary motors, the angle of the motor itself.

1.3 Classes of Brownian motors

Different types of Brownian motors have been explored in the literature, including the Feynman ratchet [24], the Landauer blowtorch [25], thermal ratchets [19], time dependent potentials [18, 20] and biological motors [13, 16]. Here we will discuss these different classes of Brownian motors and their relationship to the project.

1.3.1 Feynman ratchet and pawl

The Feynman ratchet; initially discussed in the Feynman lectures [24], is an intuitive picture of how a motor may work at the microscopic scale. This motor

was at first thought to be able to achieve Carnot efficiency, however closer analysis showed that this was not possible [26]. The system works as follows, we have two boxes thermally insulated from one another that are connected by an axle which can rotate as shown in Figure 1.3. These two boxes are at temperature T_1 and T_2 where in general $T_1 \neq T_2$. In one box there is a ratchet and pawl connected to the axle that makes it easy for the axle to turn one way (say clockwise), but hard to turn the other way (anti-clockwise). In the other box the axle is connected to vanes that are being buffeted by a gas. The motion of the vanes are random since they are dictated by Brownian motion, so the purpose of the ratchet and pawl is to rectify the Brownian motion of these vanes. One may think that this could be used to extract energy from the environment even when $T_1 = T_2$ (for example by using the axle to lift a weight). The problem is that the ratchet and pawl themselves will also be subject to random motion so sometimes the pawl will be lifted allowing the axle to turn anti-clockwise therefore the system will make no net progress, this occurs despite the asymmetry of the ratchet.

In the case where $T_2 > T_1$, the vanes will be moving quite frequently and work can be extracted from the system. Feynmann reasoned that when $T_2 > T_1$, the system could achieve Carnot efficiency in the quasi-static limit where the net motion goes to zero, this is in close analogy to a macroscopic heat engine. However the reasoning turned out to be flawed. The flaw in Feynmann's reasoning was that he did not consider the intrinsic irreversibility of the system. One must note that although the two boxes may be thermally insulated, they will still exchange heat through the axle itself. In order for Carnot's efficiency to be realized, the process must be reversible, so Feynmann's ratchet cannot attain Carnot efficiency. Modeling the Feynman ratchet and measuring its efficiency requires two degrees of freedom [27]. This is beyond the scope of this project because we will only simulate systems with one degree of freedom.

1.3.2 Landauer's blowtorch
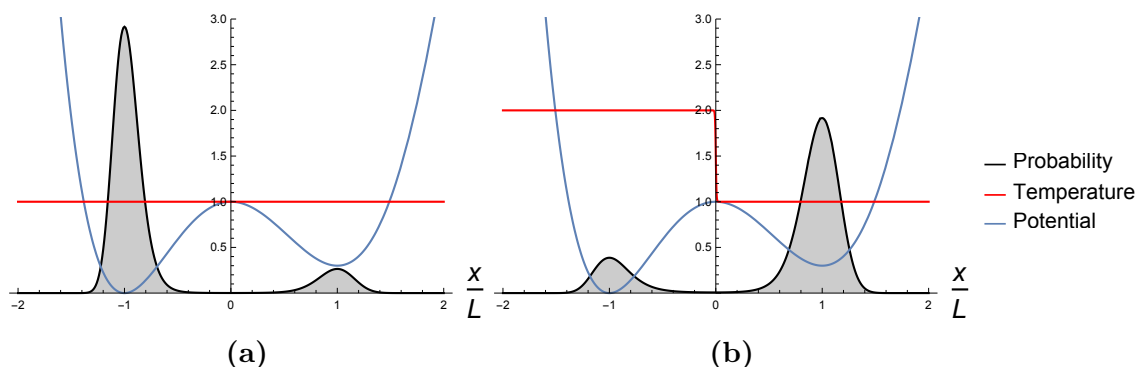
Figure 1.4: Landauer's blowtorch in a bi-stable potential. (a) we see that if the particles are left for a long enough time, then they will reach an equilibrium where the population in the upper well is less than that in the lower well. In (b) we see that if the temperature in the upper well is lower than that of the lower well, then the equilibrium concentrations are drastically altered.

The Landauer blowtorch scheme involves a temperature that varies in space [25]. The principle is shown schematically in Figure 1.4. In this figure the temperature is held fixed by an external heat source and can be made to vary along the potential. The steady state probability distribution was calculated using techniques that are described in § 3.1. In reference to this phenomena Landauer says that [25] "The relative occupation of competing states of local stability is not determined solely by the characteristics of the locally favored states, but depends on the noise along the whole path connecting the competing states." The reason that particles move against the potential gradient is that where the potential is heated, the particles become more agitated, therefore we should expect that the probability of finding a particle in a hot region is small. A common analogy due to G. E. Hinton is pebbles on a driveway. If one places pebbles on a driveway in a uniform fashion, then after some time one will find that the pebbles will pile up on the side of the driveway where there is no traffic. This occurs despite the fact that the car exerts no net sideways force on the pebbles, the explanation of this phenomena is that the car is agitating the pebbles in the center effectively at random, but once the pebbles leave the center they experience no agitation (zero temperature), so they will stay in place. This has caused some authors to describe the temperature as an effective potential [11, 28]. In particular Ref [29] report a so called reverse Landauer blowtorch effect. In their paper, the authors report that if one begins with particles in the upper well of a bi-stable potential, then as the particles move to the lower well, they will reduce the temperature of the upper well. In § 4.1, we will discuss the reverse Landauer blowtorch in more detail. The Landauer blowtorch is an important system because it clearly demonstrates that temperature gradients in stochastic systems need to be accounted for.

1.3.3   Tilted periodic potentials and molecular motors

The tilted periodic potential (Figure 1.2) is of particular interest for this project because it can be used to model biological motors [13, 16]. One way to model Brownian motors of this class is to think of a reaction coordinate x that describes the conformation of a molecule in a chemical reaction. An example of this is the reaction ATP $\rightleftharpoons$ ADP + P, where ATP is adenosine triphosphate, ADP is adenosine diphosphate and P is a lone phosphate molecule. This reaction coordinate is then coupled to a mechanical coordinate y so that each time that a reaction takes place, the motor will move in some way. Since this is a chemical reaction, the free energy will be decreased as time moves forwards. So a system that has a potential that is periodic in x is not sufficient to describe this situation, we will need to "tilt" the potential by adding a forcing f. The value of f will depend on the how far out of equilibrium the reaction is. It is shown in [13] that this can be modeled by the two dimensional Smoluchowski equation. In this project we will only be modeling the one dimensional Smoluchowski equation, so we will have to consider the case where x and y are tightly coupled. An example of tight coupling is the kinesin motor [16] that is used in cells to transport molecules. The kinesin motor is strongly bound to a track that it "walks" along. Each time that the motor takes a step it will hydrolyze an ATP molecule using the reaction shown above. This reaction liberates about

$12k_BT$ Joules of energy that the motor uses to move forward. Kinesin motors are able to take many steps forward while taking few steps backwards [30]. To overcome a barrier, a molecule needs to absorb heat from the environment, it then releases this heat as it goes down the other side. This illustrates the importance of heat interactions with the environment.

1.4   Aims

The aims of this project are as follows:

- Determine a consistent physical description of Brownian dynamics involving self-induced temperature gradients. This description must be consistent with the laws of thermodynamics and should be consistent with previous models in limiting cases.

- Develop analytical and numerical methods for solving the system.

- Explore the behavior of this system and determine the effect of self-induced temperature gradients on Brownian dynamics.

These goals are imperative in the Brownian dynamics of colloidal particles as well as the behavior of molecular motors. It is possible that one day somebody could make a molecular motor that achieves the amazing efficiency observed in biology. We believe that a solid theoretical framework will be at the center of such progress. This project is a small part of the very large theoretical framework that can be used to describe Brownian dynamics [1, 3, 16, 17].

1.5   Student contributions

The project began with a preliminary version of equations 2.6 and 2.7 suggested by Dr. Michael Jack as well as an intuitive picture that self-induced temperature gradients should have an effect on Brownian dynamics. Using physical arguments described throughout the text, these equations were modified to make a self consistent model. Through a literature review, a way to model self-induced temperature gradients was developed using ideas from a set of articles by Streater [7–10]. The numerical methods explained in §3.2 were implemented from scratch, the code can be found at https://github.com/JackDevine/Honours2016.

Chapter 2

Setting up the system

> The law that entropy always increases, holds, I think, the supreme position among the laws of Nature. If someone points out to you that your pet theory of the universe is in disagreement with Maxwell's equations — then so much the worse for Maxwell's equations. If it is found to be contradicted by observation — well, these experimentalists do bungle things sometimes. But if your theory is found to be against the second law of thermodynamics I can give you no hope; there is nothing for it but to collapse in deepest humiliation.

> **Arthur Eddington**
> **– The nature of the physical world (1928)**

2.1   The Smoluchowski equation

Here we would like to explain our model for Brownian dynamics with self-induced temperature gradients. If we know the temperature as a function of space and time, then we can use the Smoluchowski equation (equation 1.3) to model the motion. One can interpret the relation between equation 1.3 and Figures 1.2, 1.4 as follows: Brownian particles are subject to a given potential and are agitated by local thermal noise. These agitations can give the particles the energy to move over barriers created by the potential. As one could imagine, these thermal interactions draw energy from the environment as noted in Figure 1.1. One may imagine that these interactions could cause the temperature of the environment to change. Normally two simplifying (not always explicit) assumptions are made at this point [2]. (i) That the temperature gradients created by the motor are very small compared to the thermal energy of the surrounding environment which is assumed to be effectively infinite and (ii) that when these temperature fluctuations do occur, they diffuse away so rapidly that they do not need to be accounted for. In this project, we will question the second assumption and explore the consequences of not making this assumption.

First, we should derive the heat produced by the Brownian particle as it evolves on a potential, which is done in Ref [27]. Here we will reproduce the derivation because it is very important. Notice that the potential energy of the motor constrained

to a domain Ω is given by $U = \int_\Omega P(x, t)V(x)dx$. Differentiating with respect to time, we get

$$\frac{dU}{dt} = -\int_\Omega \frac{\partial J(x, t)}{\partial x}V(x)dx \tag{2.1}$$

$$= -[J(x)V(x)]_{\partial\Omega} + \int_\Omega J(x, t)\partial_x V(x, t)dx \tag{2.2}$$

The first term can be interpreted as the work done on the particle and the integrand in the second term is the local heat flux produced by the particle which we will write as $\dot{q}(x, t)$. Now that we know the heat being produced by the particle, we are ready to quantify the self-induced temperature gradients. First of all, note that if there are no sources of heat, then the temperature will evolve according to the equation

$$\frac{\partial T(x, t)}{\partial t} = D\frac{\partial^2 T(x, t)}{\partial x^2}, \tag{2.3}$$

which is the heat equation for an incompressible stationary fluid. D is the thermal diffusivity of the environment, throughout this project we will consider D to be constant. Equation 2.3 will cause any temperature gradients to diffuse with time. As we have mentioned, the movement of the Brownian particle acts as a source of heat, by adding this heat to equation 2.3 we get

$$\frac{\partial T(x, t)}{\partial t} = -\kappa\dot{q}(x, t) + D\frac{\partial^2 T(x, t)}{\partial x^2}. \tag{2.4}$$

The combination of equations 1.3 and 2.4 represent the physical coupling of temperature gradients to Brownian motion. The majority of the effort expended in this thesis will be in understanding the nature of these two coupled partial differential equations. Let us reiterate these equations here so that they can be understood in full and so that they can be referred to later. The system is written as

$$J(x, t) = -\gamma^{-1}\left[\frac{\partial V(x)}{\partial x}P(x, t) + k_B T(x, t)\frac{\partial P(x, t)}{\partial x}\right], \tag{2.5}$$

$$\frac{\partial P(x, t)}{\partial t} = -\frac{\partial J}{\partial x}, \tag{2.6}$$

$$\frac{\partial T(x, t)}{\partial t} = -\kappa\dot{q}(x, t) + D\frac{\partial^2 T(x, t)}{\partial x^2}, \tag{2.7}$$

where

- $P(x, t)$ is the probability density as a function of reaction coordinate x and time t

- $J(x, t)$ is the probability current

- γ is the friction coefficient

- $V(x)$ is the potential for the motor

- k_B is the Boltzmann constant

10

- $\dot{q}(x, t) = \partial_x V(x, t) J(x, t)$ is the local heat from the motor

- κ dictates how much the motor effects the environment. In § 2.3 we will show that κ is one over the specific heat of the environment

- D is the thermal diffusivity

Equation 2.6 is called the Smoluschowski equation which we noted earlier and equation 2.7 is the heat equation. These equations make our intuitive notions more precise, we see that the first term on the right hand side of the Smoluchowski equation (equation 2.6) is a drift term that is forced by our potential and that the second term contains a diffusion term that is scaled by our temperature.

Intuitively, the first term in equation 2.7 will create temperature gradients and the second term will cause these temperature gradients to flatten out. If the first term dominates, then the temperature gradients will grow to a very large size. In this case, we have to concede that our model will no longer be relevant. In particular our model does not include phase changes, so at the very least we require that the temperature gradients do not cause the fluid that the particle is in to freeze. This can be done if one makes sure that the second term is not significantly smaller than the first. In § 2.4 we will show that this puts a restriction on the characteristic energy of the potential. On the other hand, if the second term completely dominates, then any temperature gradients created by the Brownian particle will immediately diffuse away. In this regime, equation 2.7 will not have an effect on the evolution of the system and the model will be reduced to the Smoluchowski equation by itself. The regime that we are interested in is the regime where the first and second terms are both important. In this regime the Brownian particle will have an effect on the environment but this effect will not cause the system to behave in a way that causes our model to break down.

One may notice that the system above is a non-linear system of equations, if one looks at the last term of 2.5, then one will find that the second spatial derivative of $P(x, t)$ is multiplied by the temperature, which due to equation 2.7 is a function of $P(x, t)$. Because of this, equation 2.5 is a second order non-linear equation. Likewise if one looks at the first term of equation 2.7, then one will find that the temperature is multiplied by the first derivative of the probability distribution (which is a function of temperature), therefore equation 2.7 is also non-linear. Because we are dealing with non-linear equations, we must take extra care when finding their solutions numerically. In § 3.2 we will discuss the techniques used to solve the equations as well as analytical and convergence tests that we used to test the performance of these numerical techniques.

Temperature gradients that are self induced in Brownian dynamics have been known for some time. A particularly interesting example is the Soret-Dufour effect [32–35]. In this effect, the diffusion of the concentration of a species of molecules causes a measurable temperature effect. Another interesting example is the reverse Landauer blowtorch [29], where a nett force displacing a Brownian particle can create a temperature gradient. This, however, is in contrast to the forward Landauer blowtorch where a temperature gradient creates a psuedo-force on the particles. We will explore the reverse Landauer blowtorch in subsection 4.1.2 where we discuss how our model adds to previous work.

2.2 Boundary conditions

Equations 2.6 and 2.7 model a system that is embedded in a much larger environment. In order to talk about solutions to these equations one must define how the system interacts with the environment at the boundaries. In this project, we will discuss the following types of boundary conditions.

- Dirichlet: The value of the solution is specified at the boundaries

- Neumann: The value of the first derivative of the solution is specified at the boundaries

- Periodic: The value at the boundaries is not specified, but the left and right boundaries must take on the same value

Each type of boundary conditions comes along with its own physical interpretation, first we will deal with the boundary conditions imposed on the probability distribution.

If the potential goes to infinity at the boundaries, then the probability distribution must vanish at the boundaries. There are some potentials that are periodic where the value of the potential is the same finite number at both sides. In this case it can be interesting to apply periodic boundary conditions to the probability distribution. Physically this corresponds to a system where a particle passing through the left side will appear at the right side and vice-versa. One can picture this by imagining a particle constrained to a circular domain. The other type of boundary condition that we impose on the probability density is that the value of the density is zero at the boundaries. Mathematically, this is a special case of Dirichlet boundary conditions, physically this corresponds to so called reflecting boundary conditions [11]. Reflecting boundary conditions correspond to the physical situation where a particle is strongly constrained to a region, this could occur if a barrier that the particle cannot pass through is placed at the boundaries on either side of the domain. One can also achieve reflecting boundary conditions by making the potential go to infinity at the boundaries.

As for the temperature, both Neumann and Dirichlet boundary conditions are realized. In the case of Neumann boundary conditions, the derivative is set to zero at both boundaries. This is a very interesting case to imagine, because the derivative of the temperature physically represents the flow of heat in our system, therefore the physical interpretation of a vanishing derivative at the boundary is that no heat is flowing through the boundaries, or in other words the system is enclosed in a perfectly insulating box. If in addition there is no probability flowing out of the boundaries then energy is conserved and Neumann boundary conditions correspond to a closed system that is completely unaffected by the rest of the universe.

The second type of boundary condition that can be imposed on the temperature is the Dirichlet type where the temperature is held fixed at both boundaries. The physical interpretation of this requirement is that the domain is embedded in a much larger system that is at a fixed temperature. The tacit assumption made is that no matter what the system does, it is not able to affect the temperature of the environment. Since heat is flowing through the boundaries, the local energy of the

system is not conserved. In § 2.3 we will quantify the energy flowing through the boundaries and show that the first law of thermodynamics is upheld.

2.3   System thermodynamics

Equation 2.6 and equation 2.7 define equations of motion for our system, the system may be confined to a region Ω embedded in a larger environment which interacts with our system through the boundary conditions. In this section, we will show that our equations of motion obey the first and second laws of thermodynamics under certain conditions.

In the over-damped limit, the kinetic energy of the Brownian particle is negligible, therefore the energy of the system is completely described by the potential energy of the particle plus the thermal energy of the bath. The potential energy of the particle is $U_P = \int_\Omega V(x)P(x)dx$ and if the fluid that we are in is incompressible, then the thermal energy of the bath is $c_p \int_\Omega T(x)dx$, where c_p is the specific heat capacity of the environment. To see that this is the thermal energy consider the units of the quantity $c_p T(x, t)$. These are J K^{-1} K, so $c_p T(x, t)dx$ is the heat content of an infinitesimal element dx. With this we have the total energy of the system as

$$E(t) = \int_\Omega V(x)P(x,t)dx + c_p \int_\Omega T(x,t)dx. \tag{2.8}$$

By using the Smoluchowski equation and the heat equation, we can differentiate with respect to time to get

$$\frac{dE}{dt} = \int_\Omega V(x)\frac{\partial P}{\partial t}dx + c_p \int_\Omega \frac{\partial T}{\partial t}dx \tag{2.9}$$

$$= -\int_\Omega V(x)\frac{\partial J}{\partial x} + c_p \int_\Omega -\kappa J(x)\frac{\partial V}{\partial x} + D\frac{\partial^2 T}{\partial x^2}dx \tag{2.10}$$

$$= [V(x)J(x)]_{\partial\Omega} + \int_\Omega \frac{\partial V}{\partial x}J(x)dx - \kappa c_p \int_\Omega \frac{\partial V}{\partial x}J(x)dx + c_p D\left[\frac{\partial T}{\partial x}\right]_{\partial\Omega}. \tag{2.11}$$

Notice that the middle two terms need to cancel for the change in energy to equal the flow of energy through the boundaries. Therefore, the first law of thermodynamics requires that $\kappa = \frac{1}{c_p}$. Physically we can understand this by looking at the first term of equation 2.7. When the heat capacity is small, κ becomes large and in this case, even a small amount of heat being produced by the Brownian particle will have a large effect on the evolution of the temperature. Conversely, if the heat capacity is large, then the heat produced by the Brownian particle will have a very small effect on the temperature. We therefore expect that equation 2.7 can be neglected in the case where the environment has a very large heat capacity compared to the heat being produced by the Brownian particle.

For the entropy of the total system, we have [8]

$$S(t) = -k_B \int_\Omega P(x,t)\log(P(x,t))dx + c_p \int_\Omega \log(T(x,t))dx. \tag{2.12}$$

The first term is the Gibbs entropy in the continuous case [36] and the second term is the entropy of an incompressible fluid [37]. Using the entropy of an incompressible

fluid restricts the sytems that can be modeled by our equations of motion. In particular, we will not be able to treat Brownian particles suspended in a gas since a gas is compressible by defintion. The goal of this project is not to create a system that models many different situations in nature, but rather to create a system that is self-consistent.

Differentiating the entropy with respect to time and using equations 2.6 and 2.7, we get

$$\frac{dS}{dt} = k_B \int_\Omega \frac{\partial J}{\partial x} + \frac{\partial J}{\partial x} \log P \ dx + c_p \int_\Omega \frac{1}{T} \left(-\kappa J \partial_x V + c_p D \frac{\partial^2 T}{\partial x^2} \right) dx \quad (2.13)$$

$$= k_B \left([J]_{\partial\Omega} + [J \log P]_{\partial\Omega} - \int_\Omega \frac{J}{P} \frac{\partial P}{\partial x} dx \right) - \int_\Omega \frac{J}{T} \frac{\partial V}{\partial x} + c_p D \int_\Omega \frac{1}{T} \frac{\partial^2 T}{\partial x^2} dx. \quad (2.14)$$

Denoting the boundary terms as $B(t) = k_B([J \log P]_{\partial\Omega} + \left[\frac{\partial J}{\partial x} \right]_{\partial\Omega})$, we can write:

$$\frac{dS}{dt} = - \int_\Omega k_B \frac{J}{P} \frac{\partial P}{\partial x} + \frac{J}{T} \frac{\partial V}{\partial x} dx + c_p D \int_\Omega \frac{1}{T} \frac{\partial^2 T}{\partial x^2} dx + B(t) \quad (2.15)$$

$$= \gamma \int_\Omega \frac{J^2}{TP} dx + c_p D \int_\Omega \frac{1}{T} \frac{\partial^2 T}{\partial x^2} dx + B(t), \quad (2.16)$$

where in the second equality we used the definition of J given by 2.5.

By noticing that

$$\frac{\partial}{\partial x} \left(\frac{1}{T} \frac{\partial T}{\partial x} \right) = -\frac{1}{T^2} \left(\frac{\partial T}{\partial x} \right)^2 + \frac{1}{T} \frac{\partial^2 T}{\partial x^2}, \quad (2.17)$$

we can rewrite the second term of equation 2.20 as:

$$c_p D \int_\Omega \frac{1}{T} \frac{\partial^2 T}{\partial x^2} dx = c_p D \int_\Omega \frac{\partial}{\partial x} \left(\frac{1}{T} \frac{\partial T}{\partial x} \right) + \frac{1}{T^2} \left(\frac{\partial T}{\partial x} \right)^2 dx \quad (2.18)$$

$$= c_p D \int_\Omega \frac{1}{T^2} \left(\frac{\partial T}{\partial x} \right)^2 dx + c_p D \left[\frac{1}{T} \frac{\partial T}{\partial x} \right]_{\partial\Omega}. \quad (2.19)$$

Define

$$\dot{S}_{gen} \equiv \int_\Omega \gamma \frac{J^2}{TP} + c_p D \frac{1}{T^2} \left(\frac{\partial T}{\partial x} \right)^2 dx \quad (2.20)$$

$$(2.21)$$

so the change in entropy can be written as:

$$\frac{dS}{dt} = \dot{S}_{gen} + B(t) + c_p D \left[\frac{1}{T} \frac{\partial T}{\partial x} \right]_{\partial\Omega}. \quad (2.22)$$

We notice that the change in entropy is equal to a positive number $\dot{S}_{gen}$ plus the entropy flowing through the boundaries, this is precisely the second law of thermodynamics. Furthermore, the generated entropy in equation 2.20 can be split into two

14

terms. The first term is to be interpreted as the entropy generated by the Brownian particle; since the motion of the particle is random, as the Brownian particle diffuses we will become less certain of its position. The second term is the entropy generated by the diffusion of temperature gradients; if one studies the solutions to the heat equation, then one will find that any spikes in the temperature will flatten out and eventually the temperature will be uniform. This flattening out of the temperature is irreversible and is therefore associated with an increase in entropy. When one discusses heat engines implemented on the molecular scale, one finds that the Carnot efficiency can only be attained when the entropy generation is zero. Simply by reading equation 2.20, we can see that this occurs when the current is zero and the temperature is flat. In § 3.1 we will show that this is not possible for a Brownian particle in a tilted potential.

Some authors write the current in the form of equation 2.34, however if we use this definition of J, then $\dot{S}_{gen}$ is not necessarily positive, in fact with this term in the equation $\dot{S}_{gen}$ becomes:

$$\dot{S}_{gen} \equiv \int_\Omega \gamma \left(\frac{J^2}{TP} - \frac{J}{T} \frac{\partial T}{\partial x} \right) + c_p D \frac{1}{T^2} \left(\frac{\partial T}{\partial x} \right)^2 dx. \qquad (2.23)$$

With this version of the current, we can get local decreases in entropy, therefore we do not use this version of the current. Our version of the current is supported by Streater [7–10] and reduces to the other version in the case of constant temperature.

2.4   Making the equations dimensionless

Upon viewing equations 2.6 and 2.7, we see that there is a large number of constants that are set by the properties of the Brownian particle that we are modeling. We would like to reduce the number of variables for two reasons: (i) By reducing the number of variables we will hopefully gain a more concise physical description of the system; and (ii) Having a small number of free variables is very convenient for creating a program to approximate the equations numerically and dimensionless equations tend to be less prone to numerical error because they avoid cases where small numbers are compared to large ones in a floating point system. Here we will non-dimensionalize the equations. To do this, introduce $\hat{x} = \frac{x}{L}$, where L is the length scale of the system, the Smoluchowski equation now becomes

$$\frac{\partial P}{\partial t} = \gamma^{-1} \frac{1}{L^2} \frac{\partial}{\partial \hat{x}} \left(P \frac{\partial V}{\partial \hat{x}} + k_B T \frac{\partial P}{\partial \hat{x}} \right). \qquad (2.24)$$

Now let E_0 be the characteristic energy of the system, for a chemical reaction, E_0 will be the ΔG of the reaction and for a periodic potential, E_0 will be amplitude of the oscillations. Now we introduce the dimensionless potential and the dimensionless temperature as $\hat{V}(x) = \frac{V(x)}{E_0}$ and $\hat{T}(x) = \frac{k_B T(x)}{E_0}$ respectively. Now the Smoluchowski equation becomes

$$\frac{\partial P}{\partial t} = \frac{E_0}{\gamma L^2} \frac{\partial}{\partial \hat{x}} \left(P \frac{\partial \hat{V}}{\partial \hat{x}} + \hat{T} \frac{\partial P}{\partial \hat{x}} \right). \qquad (2.25)$$

Let $\hat{t} = \frac{E_0}{\gamma L^2} t$ and $\hat{P} = LP$, with this we have

$$\frac{\partial \hat{P}}{\partial \hat{t}} = \frac{\partial}{\partial \hat{x}} \left(\hat{P} \frac{\partial \hat{V}}{\partial \hat{x}} + \hat{T} \frac{\partial \hat{P}}{\partial \hat{x}} \right). \tag{2.26}$$

Defining $\hat{J} = \frac{\gamma L^2}{E_0} J$, applying these definitions to the equation for the temperature evolution, we find that

$$\frac{E_0^2}{\gamma k_B L^2} \frac{\partial \hat{T}}{\partial \hat{t}} = -\kappa \frac{E_0}{\gamma L^2} \hat{J}(\hat{x}) \frac{E_0}{L} \frac{\partial \hat{V}}{\partial \hat{x}} + \frac{D E_0}{k_B L^2} \frac{\partial^2 \hat{T}}{\partial \hat{x}^2}. \tag{2.27}$$

Now let

$$\alpha = \frac{\kappa k_B}{L} \quad \text{or} \quad \alpha = \frac{k_B}{c_p L} \tag{2.28}$$

$$\beta = \frac{D\gamma}{E_0}, \tag{2.29}$$

then we have

$$\frac{\partial \hat{T}}{\partial \tau} = -\alpha \hat{J}(\hat{x}) \frac{\partial \hat{V}}{\partial \hat{x}} + \beta \frac{\partial^2 \hat{T}}{\partial \hat{x}^2}. \tag{2.30}$$

As for the energy of the system, the dimensioned equation is

$$E(t) = \int P(x) V(x) dx + \frac{1}{\kappa} \int T(x) dx \tag{2.31}$$

Defining $\hat{E}(t) = \frac{E(t)}{E_0}$, we have

$$\hat{E}(t) = \int \hat{P} \hat{V} d\hat{x} + \frac{L}{k_B \kappa} \int \hat{T} d\hat{x} \tag{2.32}$$

$$= \int \hat{P} \hat{V} d\hat{x} + \frac{1}{\alpha} \int \hat{T} d\hat{x}. \tag{2.33}$$

So our system depends on the parameters α and β as well as the shape of the potential. Physically, α represents how much the particle interacts with the local environment and β represents how quickly the temperature gradients diffuse. As the length scale of the system increases, α will decrease, therefore the temperature gradients become negligible for large systems. We interpret this as meaning that the temperature gradients are much smaller than the system and can diffuse away quickly. As the characteristic energy of the system increases, β will decrease meaning that the diffusion of temperature will be negligible. We interpret this as meaning that for high energy systems, temperature gradients are created much faster than they can be diffused away. From now on when we refer to the dimensionless equations, we will omit the hats for notational convenience.

2.5   A brief discussion of the model

We are now in a position that we may discuss the physics of the equations of motion in some detail. In particular we would like to discuss the assumptions that

have to be made in order for the equations to be valid. These assumptions have been explained sporadically throughout the text and we would like to compile them into a short list that the reader should keep in mind throughout the remainder of the thesis.

1. The degrees of freedom of the bath operate at a time scale much faster than that of the Brownian particle itself

2. The kinetic energy of the particle is negligible (over-damped limit)

3. There is only one Brownian particle in our model

4. The fluid that the particle is in is incompressible

5. The fluid that the particle is in is not flowing

6. The temperature gradients are small enough that they do not induce a phase change

These assumptions have been discussed in the text, we can take any of these phenomena into account by making changes to our equations of motion, however these small changes to the equation of motion can cause the system to become very complex. Having said that, some of the assumptions made turn out to be more reasonable than one may have thought on first sight. Assumptions 1 and 2 are assumptions that are made when deriving the Smoluchowski equation from the Langevin equation, these assumptions have been discussed at length and turn out to be very reasonable [1, 2, 5, 11, 31]. Meanwhile, assumption 3 means that we cannot talk about the very interesting cooperative effects that occur in motors such as myosin, however this assumption is fine for motors such as kinesin or for colloidal particles in a potential, both of which are very interesting single particle phenomena [16]. Assumption 5 is perfectly fine in water which is the fluid of choice for all biological molecular motors. Assumption 6 is fine as long as we do not have significantly large temperature gradients. Finally assumption 7 just puts a restriction on the parameters that we choose in our simulations. As far as we are aware, there are no experimentally realized examples of Brownian particles creating a phase change in the fluid that they are suspended in.

In fluid dynamics, equation 2.7 is called the heat equation, in our case we have neglected the term that represents the flow of the fluid that the Brownian particle is situated in. Including this flow would involve adding $u(x)\frac{\partial T}{\partial x}$ to the left hand side of equation 2.7, where $u(x)$ is velocity of the flow of the fluid. The role of fluid dynamics is discussed further in § 6.3. Here we will note that the assumption that the fluid is stationary ($u(x) = 0$) means that the temperature gradients cannot be allowed to become too large because temperature gradients are known to create flows in fluids. Even though these flows may effect the validity of our model in real life we will neglect them for three main reasons. (i) They are not related to the physics that we would like to capture in this project since this is a project on statistical mechanics, not fluid dynamics. (ii) We would not like to depart too far from the explored literature, which is similar to reason (i), however here we would like to stress that our model is just an extension of previous models, extending the

extension before understanding the extension could be premature. (iii) Including the flow into our equations of motion would increase the complexity of the system to beyond the scope of an honors project: although simply adding the fluid flow to equation 2.7 may seem like an innocent operation, calculating the way in which the temperature gradients and the flow of the Brownian particle effect the fluid flow would mean adding a third equation to our already non-linear coupled system of equations.

Our model includes a temperature that depends on x and t, which has been explored in the literature [31]. Some authors write the current as [28, 31]

$$J(x,\,t) = -\gamma^{-1}\frac{\partial}{\partial x}\left(\frac{\partial V(x,\,t)}{\partial x}P(x,\,t) + k_B\frac{\partial}{\partial x}[T(x,\,t)P(x,\,t)]\right),\qquad (2.34)$$

the difference being that they put the temperature inside the inner derivative. We will return to this difference in § 2.3, where we will discuss the role that the current has in the generation of entropy. Our model departs from previous work is that the temperature now depends on the evolution of the probability distribution as well. Coupled models of this type have been mentioned earlier by Streater [7–10]. Our work uses a similar model that was modified to suit our needs.

The other restriction that we must enforce on our model is that there is only a very small number of Brownian particles. This is because the temperature gradients can act as inter-particle interactions. To see this imagine that there are two particles moving about and creating temperature gradients. If one particle moves to a location where the other has created a temperature gradient, then it will be effected by the temperature gradient created by the other particle. Therefore, to model this, one would need to model the probability distributions of each particle separately and make sure that the interactions are accounted for. We stress this point because often people will use the Smoluchowski equation to describe the density of particles in a fluid. Interpreting $P(x,\,t)$ in this way in the presence of self induced temperature gradients would neglect the inter-particle interactions and would not be an accurate description, therefore we will be careful to make sure that $P(x,\,t)$ is used to model the probability distribution of a single colloidal particle, not many.

Chapter 3

Solving the system

He who refuses to do arithmetic is doomed to talk nonsense.

John McCarthy
– Progress and it's Sustainability (1995)

Now that we have determined that our system is physical and we have made insights into the qualitative nature of our system, we must build techniques for solving the system so that we can gain quantitative insights. We will begin in § 3.1 by using analytical techniques to find stationary solutions to our equations of motion.

3.1 Steady state solution

In order to see how the equations of motion behave with time, we have to resort to numerical methods (see § 3.2). However we note that for a given potential there will be a stationary solution that we will refer to as the "steady state". In the steady state we have

$$\frac{\partial P(x,\,t)}{\partial t} = 0 = \frac{\partial J(x,\,t)}{\partial t}, \tag{3.1}$$

this implies that the current in the steady state is constant, we will denote this with J_s. In the steady state, the temperature is not changing so

$$\frac{\partial T(x,\,t)}{\partial t} = 0 = -\kappa J_s \partial_x V(x,\,t) + D\frac{\partial^2 T(x,\,t)}{\partial x^2}. \tag{3.2}$$

In one dimension, equation 3.2 can be written as an ordinary differential equation of the form

$$T''(x) = \frac{\kappa J_s}{D} V'(x) \tag{3.3}$$

We can solve this equation by integrating both sides twice to give

$$T(x) = \frac{\kappa J_s}{D} \int_0^x V(x')dx' + \xi x + d, \tag{3.4}$$

19

for unknown constants ξ and d. If $J_s = 0$ then the steady state for the probability density is given by

$$P_{ss}(x) = N \exp\left(-\int_a^x \frac{V'(x')}{k_B T(x')} dx'\right) \tag{3.5}$$

and

$$T(x) = \xi x + d. \tag{3.6}$$

We can now apply boundary conditions to the temperature, these can be either Dirichlet

$$\left.\frac{\partial T}{\partial x}\right|_{\partial\Omega} = 0, \tag{3.7}$$

or Neumann,

$$T|_{\partial\Omega} = T_0. \tag{3.8}$$

In either case, $\xi = 0$ which implies that the temperature is constant. In this case equation 3.4 becomes the Boltzmann distribution

$$P(x) = N \exp\left(-\frac{V(x)}{k_B T(x)}\right). \tag{3.9}$$

An example of the Boltzmann distribution is shown in Figure 3.1, in this figure we have a confining potential causing the probability density to go to zero for large x. It is interesting to note that in the steady state, the temperature gradients become flat. This is because after enough time the diffusion term in equation 2.7 causes temperature gradients to flatten out.

Meanwhile, a tilted periodic potentials can be written as $V(x) = -fx + v_0(x)$ for some constant f and a periodic function $v_0(x)$. In this case, equation 3.4 becomes

$$T(x) = \frac{\kappa J_s}{D} \int_0^x -fx' dx' + \frac{\kappa J_s}{D} \int_0^x v_0(x') dx' + \xi x + d. \tag{3.10}$$

The first term on the right hand side of this equation will grow like x^2. The reason that the temperature is growing is because as the Brownian particle moves down the potential, it loses potential energy. This potential energy is converted into thermal energy, explaining why the temperature increases with x. We therefore conclude that the tilted periodic potential does not have a meaningful steady state.

3.2 Finite differences

In order to explore the dynamics of equations 2.6 and 2.7 we will need to resort to numerical techniques. The one dimensional equations can be solved on a discrete grid by using the finite differences method. The main idea behind this strategy is to approximate derivatives with equations of the form

$$\frac{df}{dx} \approx \frac{f(x-h) - f(x+h)}{2h}, \tag{3.11}$$
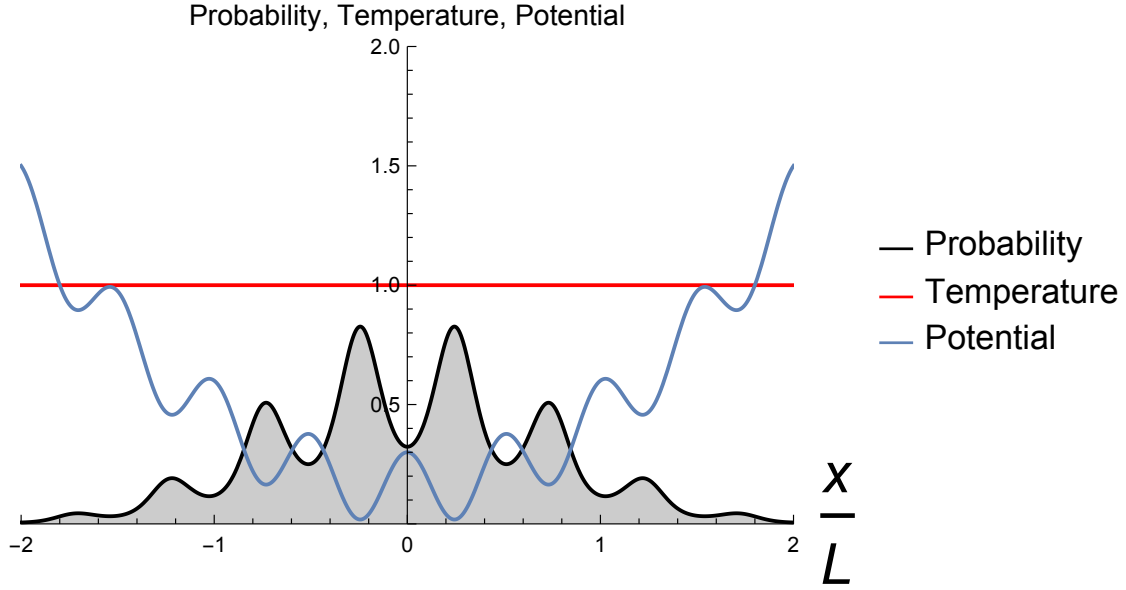
Figure 3.1: A solution of the system in the steady state with a confining potential.

for some small h, likewise the second derivative of a function is approximated with

$$\frac{d^2 f}{dx^2} \approx \frac{f(x-h) - 2f(x) + f(x+h)}{h^2}, \tag{3.12}$$

In our simulations, we will use the Crank-Nicolson scheme [38, 39] to solve the equations. From now on, we will use the notation that $F(j\Delta x, n\Delta t) = F_j^n$, the key equation for the Crank-Nicolson scheme is

$$\frac{P_j^{n+1} - P_j^n}{\Delta t} = \frac{1}{2}(F_j^{n+1} + F_j^n), \tag{3.13}$$

where F represents the right-hand side of the equation that we are doing finite differences on. Equation 3.13 represents the average of taking one Euler step forwards and on Euler step backwards. This is an implicit set of equations that we will need to solve. In particular, one may notice that F needs to be estimated at the future time in order for the equation to make sense. We will linearize the problem by assuming that the quantities of interest do not change by much in one time step.

By applying finite differences to the dimensionless Smoluchowski equation (equation 2.26), we find that:

$$F_j^i = \frac{P_{j+1}^i \partial V_{j+1}^i - P_{j-1}^i \partial V_{j-1}^i}{2\Delta x} + \frac{T_{j+1}^i - T_{j-1}^i}{2\Delta x} \frac{P_{j+1}^i - P_{j-1}^i}{2\Delta x}$$
$$+ T_j^i \frac{P_{j+1}^i - 2P_j^i + P_{j-1}^i}{\Delta x^2}, \tag{3.14}$$

where we omitted the hats for notational convenience. We make the following defi-

21

nitions:

$$a_j^{n+1} = \frac{-2T_j^{n+1}}{\Delta x^2},$$

$$b_j^{n+1} = \frac{\partial_x V_{j+1}^{n+1}}{2\Delta x} + \frac{T_{j+1}^{n+1} - T_{j-1}^{n+1}}{4\Delta x^2},$$

$$c_j^{n+1} = -\frac{\partial_x V_{j-1}^{n+1}}{2\Delta x} - \frac{T_{j+1}^{n+1} - T_{j-1}^{n+1}}{4\Delta x^2},$$

$$a_j^{n} = \frac{-2T_j^{n}}{\Delta x^2},$$

$$b_j^{n} = \frac{\partial_x V_{j+1}^{n}}{2\Delta x} + \frac{T_{j+1}^{n} - T_{j-1}^{n}}{4\Delta x^2},$$

$$c_j^{n} = -\frac{\partial_x V_{j-1}^{n}}{2\Delta x} - \frac{T_{j+1}^{n} - T_{j-1}^{n}}{4\Delta x^2}, \tag{3.15}$$

With these definitions, the Crank-Nicolson scheme can be written down as follows:

$$-\frac{\Delta t}{2}a_j^{n+1}P_{j-1}^{n+1} + \left(1 - \frac{\Delta t}{2}b_j^{n+1}\right)P_j^{n+1} - \frac{\Delta t}{2}c_j^{n+1}P_{j+1}^{n+1}$$

$$= a_j^{n}P_{j-1}^{n} + \left(1 + \frac{\Delta t}{2}b_j^{n}\right)P_j^{n} + \frac{\Delta t}{2}c_j^{n}P_{j+1}^{n}. \tag{3.16}$$

This equation can be written in matrix form by defining the following matrices

$$A = \begin{bmatrix} a_0^{n+1} & b_1^{n+1} & 0 & 0 & 0 & \dots & 0 \\ c_0^{n+1} & a_1^{n+1} & b_2^{n+1} & 0 & 0 & \dots & 0 \\ 0 & c_1^{n+1} & a_2^{n+1} & b_3^{n+1} & 0 & \dots & 0 \\ \vdots & \vdots & \ddots & \ddots & \ddots & \vdots & \vdots \\ 0 & & \dots & & c_{J-2}^{n+1} & a_{J-1}^{n+1} & b_J^{n+1} \\ 0 & & \dots & & & c_{J-1}^{n+1} & a_J^{n+1} \end{bmatrix}, \quad P^{n+1} = \begin{bmatrix} P_0^{n+1} \\ P_1^{n+1} \\ \vdots \\ P_{J-1}^{n+1} \\ P_J^{n+1} \end{bmatrix} \tag{3.17}$$

$$B = \begin{bmatrix} a_0^{n} & b_1^{n} & 0 & 0 & 0 & \dots & 0 \\ c_0^{n} & a_1^{n} & b_2^{n} & 0 & 0 & \dots & 0 \\ 0 & c_1^{n} & a_2^{n} & b_3 n & 0 & \dots & 0 \\ \vdots & \vdots & \ddots & \ddots & \ddots & \vdots & \vdots \\ 0 & & \dots & & c_{J-2}^{n} & a_{J-1}^{n} & b_J^{n} \\ 0 & & \dots & & & c_{J-1}^{n} & a_J^{n} \end{bmatrix}, \quad P^{n} = \begin{bmatrix} P_0^{n} \\ P_1^{n} \\ \vdots \\ P_{J-1}^{n} \\ P_J^{n} \end{bmatrix} \tag{3.18}$$

With these matrices, the equation now becomes,

$$\left(\mathbb{1} - \frac{\Delta t}{2}A\right) \cdot P^{n+1} = \left(\mathbb{1} + \frac{\Delta t}{2}B\right) \cdot P^{n}, \tag{3.19}$$

we interpret this equation as saying that half of a backwards Euler step acting on P^{n+1} is equal to half of a forward Euler step acting on P^n. We write the equation to step P forward one time step as

$$P^{n+1} = \frac{\mathbb{1} + \frac{\Delta t}{2} B}{\mathbb{1} - \frac{\Delta t}{2} A} P^n. \tag{3.20}$$

Each time that we step forward using this equation we will be out by a factor, this means that at each step we will need to renormalize using the equation $\int P(x) dx = 1$. If we do not apply this normalization, then the norm of our vector will change dramatically during a simulation. In order to estimate the integrals involved, we used Simpson's rule of integration.

Likewise, we can apply the Crank-Nicolson scheme to the heat equation, (eq 2.30), by looking at the right-hand side of this equation, we find that

$$F_j^i = -\alpha \left(P_j^i (\partial_x V_j^i)^2 + T_j^i \frac{P_{j+1}^i - P_{j-1}^i}{2\Delta x} \partial_x V_j^i \right) + \beta \frac{T_{j+1}^i - 2T_j^i + T_{j-1}^i}{\Delta x^2}. \tag{3.21}$$

Just like the discretized Smoluchowski equation, these equations can be written in matrix form. The temperature is normalized by assuming that the energy remains fixed, this will be true as long as no heat or current flows through the boundaries, i.e. $J(x = a) = 0 = J(x = b)$ and $\frac{\partial T}{\partial x}|_a = 0 = \frac{\partial T}{\partial x}|_b$. In this case, the energy is constant and is given by $E = \int P(x) V(x) dx + c_p \int T(x) dx$, so each time that we step the temperature forward, we have to calculate the potential and thermal energy and then scale the temperature so that the total energy remains fixed.

Fortunately the matrices that we are dealing with are very sparse, so the program used to solve these equations can save on memory by calling sparse matrix libraries.

Implementing these boundary conditions requires that we change our matrices A and B. Specifically, we will need to modify the top and bottom rows. The reason that we can do this is because a matrix represents a system of equations. The first and last rows of the matrices effect the first and last components of the vectors that we are doing finite differences on. For each boundary condition, we need to make sure that the equations represented by our first and last rows reflect our desired boundary conditions.

Dirichlet boundary conditions

Imagine that we have a $n \times 1$ vector u that we want to step forward with finite differences while keeping the first and last components of u fixed. The equation for stepping u forward is given by

$$u^{n+1} = \frac{\mathbb{1} + \frac{\Delta t}{2} B}{\mathbb{1} - \frac{\Delta t}{2} A} u^n, \tag{3.22}$$

this equation will certainly affect the first and last components of u. In order to avoid this, we need to make sure that the first and last rows of $(\mathbb{1} + \frac{\Delta t}{2} B)$ and $(\mathbb{1} - \frac{\Delta t}{2} A)$ are the same as the first and last rows of the identity matrix. One must

take care when using the energy to normalize when considering Dirichlet boundary conditions, because the energy in the system is no longer conserved. To account for this, we calculate the heat flowing through the boundaries at each step and subtract this from the energy of the system before we normalized the system.

Neumann boundary conditions

The derivative at the boundaries can be made to be zero at the boundaries by making sure that the first and last rows of our matrices represent the equations $u_J - u_{J-1} = 0$ and $u_0 - u_1 = 0$ respectively. This can be done by replacing the first row with $\{1, -1, 0, \ldots, 0\}$ and the last row with $\{0, 0, \ldots, 0, -1, 1\}$.

Periodic boundary conditions

Periodic boundary conditions state that $u_0 = u_J$, if this is true at step i, then we can make sure that it is true at step $i+1$ by modifying our matrix appropriately. To be more precise if our finite differences matrix takes the form of equation 3.17, then in order to have periodic boundary conditions we would have to modify it to read:

$$A = \begin{bmatrix} a_0^{n+1} & b_1^{n+1} & 0 & 0 & 0 & \cdots & c_0^{n+1} \\ c_0^{n+1} & a_1^{n+1} & b_2^{n+1} & 0 & 0 & \cdots & 0 \\ 0 & c_1^{n+1} & a_2^{n+1} & b_3^{n+1} & 0 & \cdots & 0 \\ \vdots & \vdots & \ddots & \ddots & \ddots & \vdots & \vdots \\ & & & & & & \\ 0 & & \cdots & & c_{J-2}^{n+1} & a_{J-1}^{n+1} & b_J^{n+1} \\ b_J^{n+1} & & \cdots & & & c_{J-1}^{n+1} & a_J^{n+1} \end{bmatrix}. \tag{3.23}$$

This is equivalent to stretching out the matrix in a periodic fashion, we note that the matrix for periodic boundary conditions cannot be written in tridiagonal form. When the matrices involved are tridiagonal, we can inform the compiler of our program so that it can used highly optimized routines for solving the equations. In the case of periodic boundary conditions, however, we simply inform the compiler that the matrices are sparse, this means that we do not get the same speed for periodic boundary conditions as we do for other boundary conditions.

All of these boundary conditions were implemented in Julia which is a high level open source language for scientific computing [40]. A function was made so that the user can decide which boundary condition that they want through a keyword argument and then the program will implement finite differences for that boundary type. An example of finite differencing with periodic boundary conditions is shown in Figure 3.2.
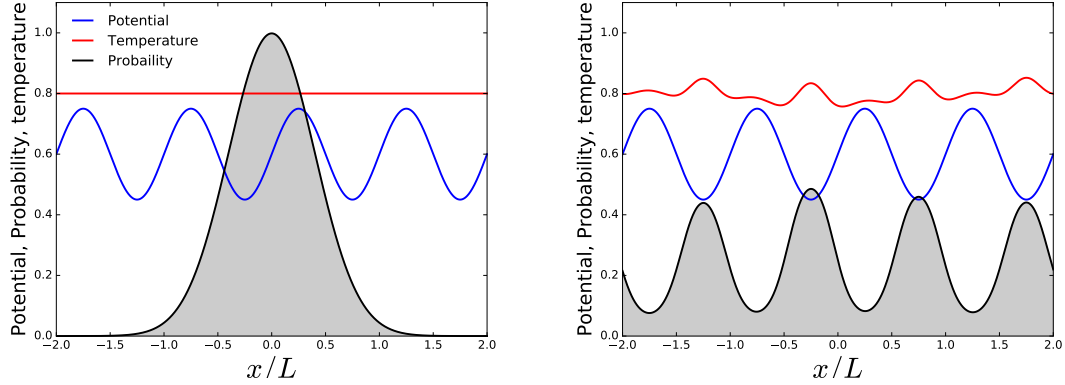
Figure 3.2: An example of a periodic system visualized in one dimension.
A simulation of equations 2.26 and 2.30 using finite differences, $\Delta t = 1 \times 10^{-4}$ and the number of points on the x-axis is 1000, all quantities are dimensionless, this simulation involved 30,000 steps. We have $\alpha = 5 \times 10^{-3}$ and $\beta = 1 \times 10^{-2}$ we are imposing periodic boundary conditions on both the temperature and the probability distribution.

3.3 Testing the numerics

The idea behind finite differences is that as the discretization size goes to zero, the numerical approximation should converge on the correct analytical solution. Here we will compare our numerics with some known analytical results as well as performing convergence tests.

3.3.1 A comparison with analytical results

For a confining potential and with $\alpha = 0$, the Smoluchowski equation (equation 2.26) has a steady state probability density given by the Boltzmann distribution Figure 3.3 shows the a simulation where we began the system in the analytically calculated steady state, we then used finite differences to step forward 50,000 steps with $\Delta t = 1 \times 10^{-4}$. After this simulation, we only found a minimal divergence from the steady state.

The heat equation (equation 2.30) can be solved using a Fourier series technique. In the case where there are no sources of heat, we have
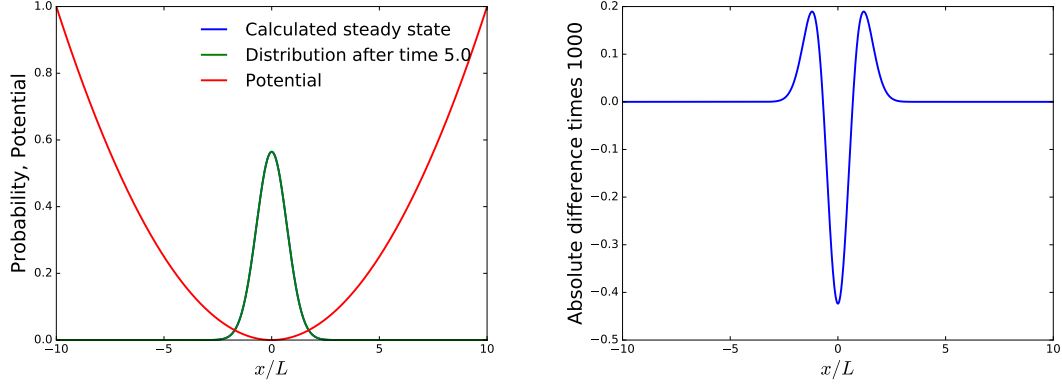
$$\frac{\partial T}{\partial t} = \beta \frac{\partial^2 T}{\partial x^2}. \tag{3.24}$$

The initial condition for the temperature will be denoted by,

$$T(x, 0) = f(x). \tag{3.25}$$

Given boundaries at $x = \pm\infty$ with vanishing $\frac{\partial T(x,t)}{\partial x}$, the time-dependent solution of the heat equation can be given as:

$$T(x, t) = \sum_{n=1}^{\infty} D_n \sin\left(\frac{n\pi x}{L}\right) \exp\left(\frac{-n^2\pi^2\beta t}{L^2}\right), \tag{3.26}$$

25

Figure 3.3: Finite differences in the steady state. The steady state for the system is given by the Boltzmann distribution, we start the system off in this state and then simulate the system forward 50,000 steps with $\Delta t = 10^{-4}$ and $\Delta x = 2 \times 10^{-2}$. (a) The analytical steady state with the state after the simulation. (b) The absolute difference between these two vectors. Even after 50,000 steps the system has not deviated from the analytical steady state significantly.

where

$$D_n = \frac{2}{L} \int_0^L f(x) \sin\left(\frac{n\pi x}{L}\right) dx. \tag{3.27}$$

Say that we begin with a Gaussian function for the temperature, such that

$$T(x,\, 0) = f(x) = \exp\left(-\frac{x^2}{4\beta}\right), \tag{3.28}$$

then as time goes on, the solution will be given by

$$T(x,\, t) = \frac{1}{\sqrt{t+1}} \exp\left(-\frac{x^2}{4\beta(t+1)}\right). \tag{3.29}$$

We can compare these analytical results to the numerical ones obtained through finite differences, this is done in Figures 3.3 and 3.4. These figures show that even after many steps, the calculated solution has not deviated from the analytical one.

3.3.2 Convergence tests

If the finite differences methods that we have implemented are correct, then as the discretization size goes to zero, the numerical approximation will converge on the correct solution to the underlying equation being approximated. In the previous section we showed that finite differences approximated the solution very closely in some instances where the analytical result could be obtained. In general, we will not have an analytical solution to compare to but we would still like to be able to quantify the performance of our techniques.

Convergence tests involve decreasing the discretization size and checking whether the numerical solutions converge at all. In Figure 3.5, the Smoluchowski equation
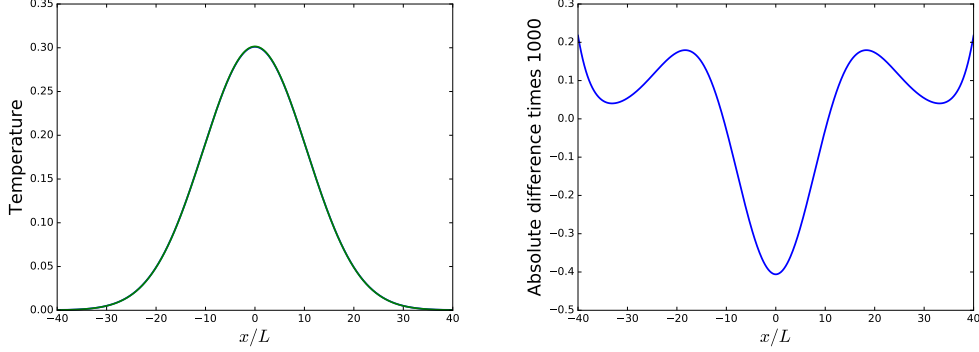
Figure 3.4: Finite differences on the heat equation. We simulate a situation where there are no sources for the heat equation and use equation 3.26 to obtain the analytical result we then compare this to the result of finite differences with $\Delta t = 1 \times 10^{-2}$ and $\Delta x = 2 \times 10^{-2}$.
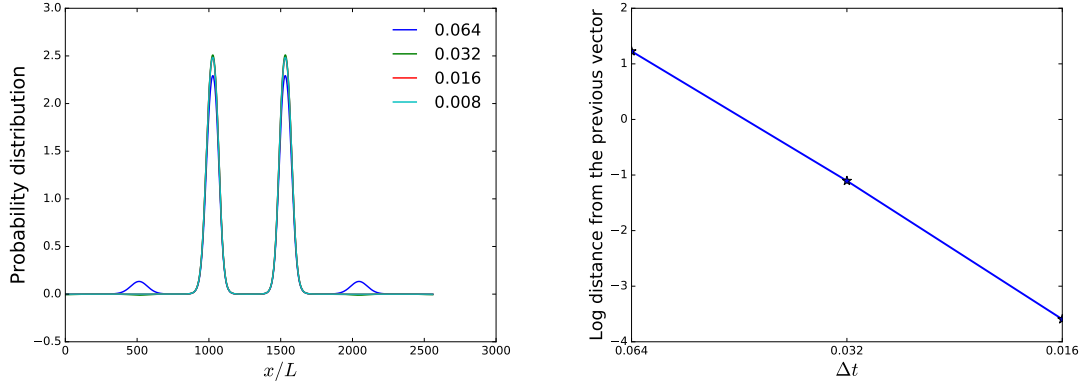
Figure 3.5: The convergence of the probability distribution. As Δt is decreased, the spatial discretization Δx is kept constant at 6×10^{-3}. (a) The Smoluchoski equation is simulated forward for 1.0 seconds each line shows the result with a different value of the time step Δt. (b) The normed difference between each of the successive vectors is calculated and the result is plotted on a log scale, the slope of this graph is called the convergence rate.
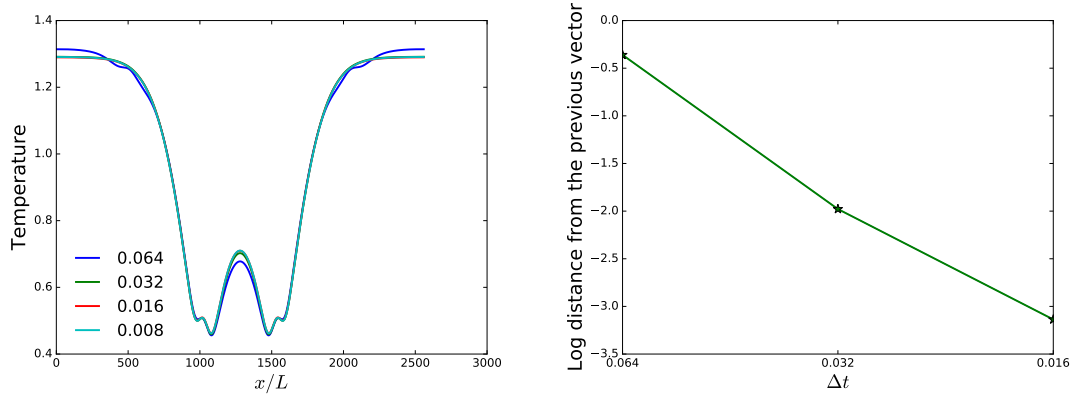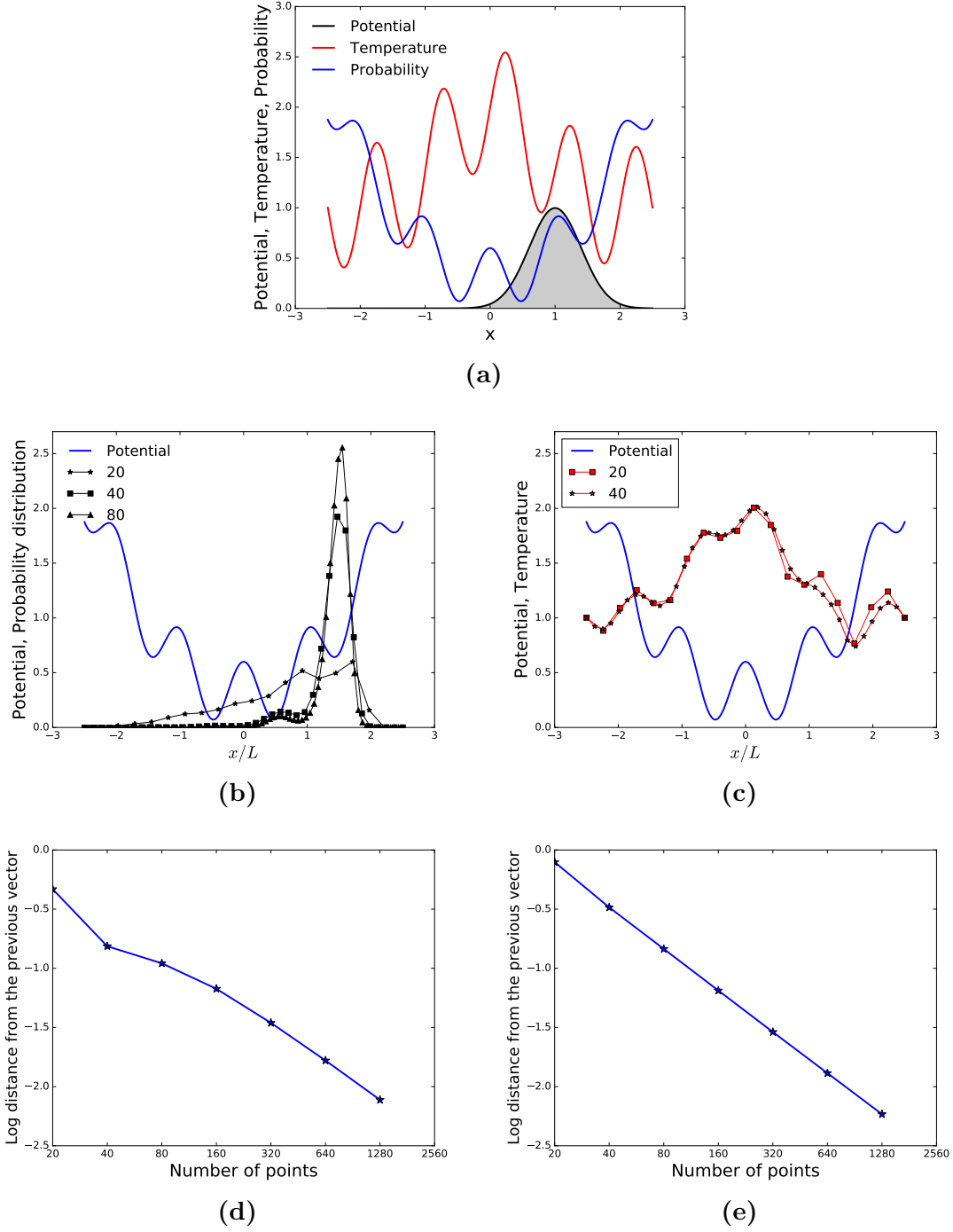
Figure 3.6: The convergence of the temperature. As Δt is decreased, the spatial discretization the number of points are kept constant at 2500. (a) the coupled equations are simulated forward for 2.0 seconds, each line shows the temperature with a different value of the time step Δt. (b) the normed difference between each of the successive vectors is calculated and the result is plotted on a log scale.

was simulated while keeping the temperature fixed, each time we halve Δt and measure the normed difference between the new result and the previous one.

Likewise, we can do convergence tests for the coupled system, for brevity we have only included the results for the evolution of the temperature. All of these plots show that the numerical solution converges exponentially. The convergence tests themselves do not prove that the numerical algorithms properly represent the equations 2.26 and 2.30, however, combined with our analytical tests, they give us confidence that the numerics do agree with the true solution.

One can also perform convergence tests by increasing the number of points, from this one learns how sensitive the numerics are to the size of the spatial discretization Δx. This is shown in Figure 3.7, here we see that the temperature converges much more rapidly than the probability distribution does, however as Δx goes down, both converge exponentially.

(a)

(b)

(c)

(d)

(e)

Figure 3.7: Convergence tests for Δx**.** Δt is held fixed at 1×10^{-5} and $\alpha = 5 \times 10^{-4}$ and $\beta = 1 \times 10^{-2}$. (a) The initial configuration of the system, both the potential and the initial temperature are chosen to be functions with large derivatives so that we can see how sensitive the numerics are to gradients. (b, c) The system after 40,000 steps forward in time, here we have not used the filling plot style to show the probability distribution so that one can see the difference between the different lines. (d) For each vector that was found through finite differences, we calculate its difference from the previous one, the x axis shows the length of each of the vectors. The y axis shows the log of these differences (e) Convergence of the temperature with an increasing number of points.

29

Chapter 4

Exploration

In that Empire, the Art of Cartography attained such Perfection that the map of a single Province occupied the entirety of a City, and the map of the Empire, the entirety of a Province. In time, those Unconscionable Maps no longer satisfied, and the Cartographers Guilds struck a Map of the Empire whose size was that of the Empire, and which coincided point for point with it. The following Generations, who were not so fond of the Study of Cartography as their Forebears had been, saw that that vast map was Useless, and not without some Pitilessness was it, that they delivered it up to the Inclemencies of Sun and Winters. In the Deserts of the West, still today, there are Tattered Ruins of that Map, inhabited by Animals and Beggars; in all the Land there is no other Relic of the Disciplines of Geography.

Jorge Luis Borges (translated by Andrew Hurley)
– "On Exactitude in Science"

Now that we have set up the framework for our system, we are able to discuss particular phenomena and their relation to nature. Here we will discuss some prototypical problems in stochastic systems and their behavior when considered in the light of equations 2.6 and 2.7. The point of this chapter is not to explain a particular experiment or the nature of a particular molecular motor in great detail. Nor is our aim to make a general model that may be easily adapted to any situation that the reader might fancy. Instead we aim to extract the physics that is at the essence of equations 2.6 and 2.7. We will find that our system differs from those previously explored, however, the previous behavior may always be recovered by taking the limit of either high specific heat capacity or fast thermal diffusivity as discussed in § 2.4.

4.1   Bistable potentials

A bistable potential has two stable minima and an intermediate unstable maximum as depicted schematically in Figure 4.1, these potentials occur in a wide range of applications including digital logic [41, 42], protein folding [43] and chemical reactions [44]. The bistable potential well is one of the simplest ways to approach the Kramers' rate and many other important properties of a stochastic system
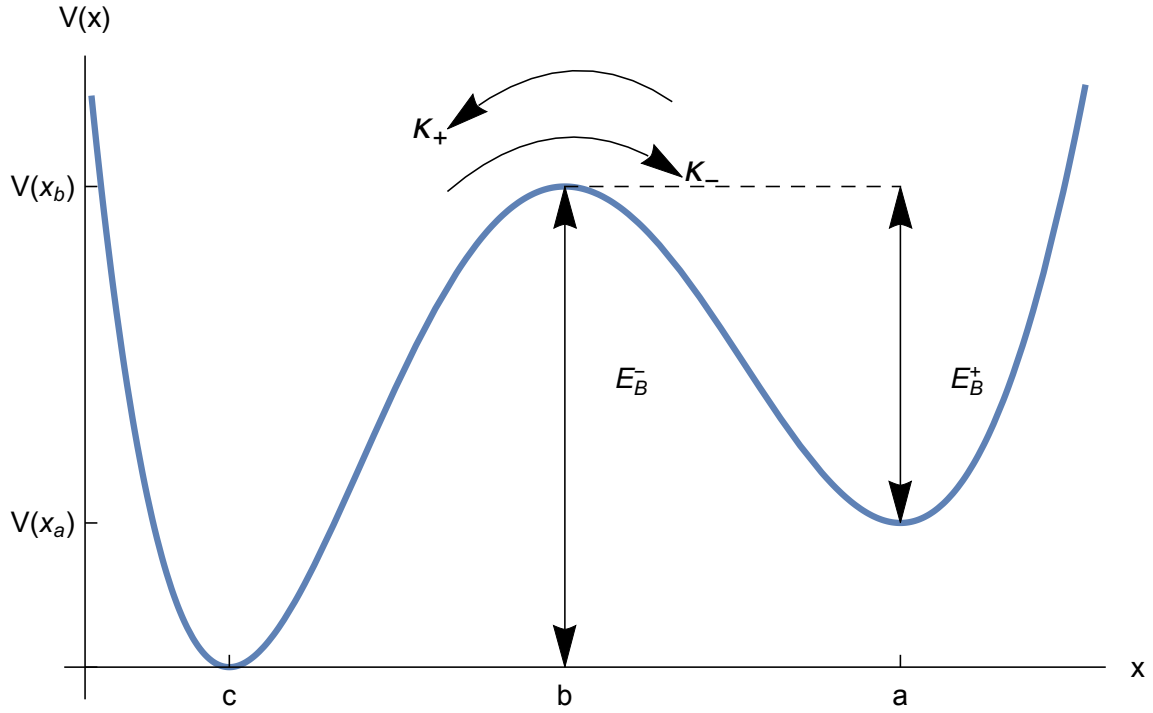
Figure 4.1: Bistable potential. In this plot we show the potential used to explore the Kramers' rate and the reverse Landauer blowtorch. The potential has local minima at a and c and a maximum at b. If we begin with a probability distribution in the upper well, then the distribution will decay into the ground state of the upper well and then begin to decay into the lower well. The rate of flow from the upper well to the lower one will be denoted by κ_+ and the rate of flow from the lower well into the upper one will be denoted by κ_-. In order for a Brownian particle to go from a to c, it will need to acquire thermal energy E_B^+, likewise to go from c to a, it will need energy E_B^-.

[41, 45, 46]. In the context of Brownian motion, understanding the nature of bistable potentials can help one to understand more complicated potentials comprised of multiple deep wells.

4.1.1 Kramers' rate

Consider the potential shown in Figure 4.1, if we begin in a state where we are certain that the particle is in the upper well, then as time passes, we should expect the probability distribution to move from point a over the barrier at b and into the well at point c. We will consider the regime where $E_B^+ = V(x_b) - V(x_a) \gg k_B T$, where T is constant, in this regime the rate at which the particles flow from a to c is given by the Eyring-Kramers' law [31, 47].

We will now derive the Kramers' rate analytically for a constant temperature, an example of this derivation involving a slightly different Fokker-Planck equation is shown in Ref [11]. Say that the particle begins at a, we are interested in knowing how long it will take to reach a point x. This function is denoted by $\tau(x)$ and is called the first passage time [11] the first passage time is associated with a probability density

$f(x, t)$. In particular, $f(x, t)$ denotes the probability that the particle has not passed the point x after a time t, given that the particle started at c. We would like to obtain the mean first passage time $\langle \tau(x) \rangle \equiv \int_0^\infty t\, f(x, t)\, dt$, to do this we consider the dimensionless form of the Smoluchowski equation with constant temperature

$$\frac{\partial P(x, t)}{\partial t} = \frac{\partial}{\partial x} \left(P(x, t) \partial_x V + T \partial_x P(x, t) \right). \tag{4.1}$$

We see that $f(x, t)$ obeys the same equation of motion as $P(x, t)$. Integrating both sides yields

$$\int_0^\infty dt \partial_t f(x, t) = \int_0^\infty dt \frac{\partial}{\partial x} \left(f(x, t) \partial_x V + T \partial_x f(x, t) \right), \tag{4.2}$$

using the fact that $f(x, \infty) = 0$ and $f(x, 0) = 1$, we find that

$$-1 = \frac{\partial}{\partial x} \left(-\langle \tau(x) \rangle \partial_x V + T \frac{\partial \langle \tau(x) \rangle}{\partial x} \right). \tag{4.3}$$

Since time dependence has been removed and we are only in one dimension, this is an ordinary differential equation for $\langle \tau(x) \rangle$. We notice that,

$$\frac{d}{dx} \left[\exp \left(-\frac{V(x)}{T} \right) \frac{d}{dx} \langle \tau(x) \rangle \right] = \frac{1}{T} \exp \left(\frac{-V(x)}{T} \right) \left(-V'(x) \frac{d}{dx} \langle \tau(x) \rangle + \frac{d^2}{dx^2} \langle \tau(x) \rangle \right) \tag{4.4}$$

therefore

$$\frac{d}{dx} \left[\exp \left(-\frac{V(x)}{T} \right) \frac{d}{dx} \langle \tau(x) \rangle \right] = -\frac{1}{T} \exp \left(-\frac{V(x)}{T} \right). \tag{4.5}$$

Integrating from $-\infty$ to x we have:

$$\exp \left(-\frac{V(x)}{T} \right) \frac{d}{dx} \langle \tau(x) \rangle = -\frac{1}{T} \int_{-\infty}^x dz \exp \left(-\frac{V(z)}{T} \right). \tag{4.6}$$

Finally, integrating from a to x and using the fact that $\langle \tau(a) \rangle = 0$, we get

$$\langle \tau(x) \rangle = \frac{1}{T} \int_a^x dy \exp \left(\frac{V(y)}{T} \right) \int_{-\infty}^y dz \exp \left(-\frac{V(z)}{T} \right). \tag{4.7}$$

Because of the shape of the potential, the value of both integrands will decay exponentially as we go out to infinity, therefore we can take the upper and lower limits of both integrals to be $\pm\infty$ respectively. This means that we can carry out the integrals using standard results for Gaussian integrals.

If the particle starts at a, then the potential in the first integrand can be approximated by the second order Taylor expansion around b and the second integrand will be approximated by an expansion around a, more explicitly

$$V(y) \approx V(b) + \frac{V''(b)}{2}(x - b)^2, \tag{4.8}$$

$$V(z) \approx V(a) + \frac{V''(a)}{2}(x - a)^2. \tag{4.9}$$

33

So for the mean first passage time of particles going from a to c we find,

$$\langle \tau_{a \to c} \rangle = \frac{2\pi}{\sqrt{-V''(b)V''(a)}} \exp\left(\frac{V(b) - V(a)}{T}\right). \tag{4.10}$$

The Kramers' rate is given by one over the mean first passage time, we will denote the rate of particles moving from a to c as κ_+, which is given by

$$\kappa_+ = \frac{\sqrt{|V''(b)V''(a)|}}{2\pi} e^{\frac{-E_B}{T}}. \tag{4.11}$$

Likewise, there will be a current flowing from c to a, we will denote this by κ_-, once we have calculated both of these rates, the population in the upper well will be given by the differential equation

$$\frac{dP_+}{dt} = -\kappa_+ P_+(t) + \kappa_- P_-(t). \tag{4.12}$$

If we start with the population situated entirely in the upper well, then we get:

$$P_+(t) = \exp\left(-(\kappa_+ - \kappa_-)t\right). \tag{4.13}$$

We can also achieve this result numerically by starting the system off in the upper well and simulating forward in time while calculating the probability that the particle is in the upper well at each step. We then fit an exponential to this data and the fitted rate will be our numerically estimated Kramers' rate. To assist with measuring the Kramers' rate, we used Hermite interpolation to create a sixth order polynomial with the desired bistable shape. Specifically, we would allow $V(x)$ to be a general 6th order polynomial and then we would specify the value of the polynomial at the locations a, b and c, we would also enforce that the first derivative vanished at these locations. This would yield 6 equations which we would solve to give us the coefficients of $V(x)$, this procedure has been automated to facilitate rapid exploration of many bi-stable potentials, an example of such a polynomial is shown in Figure 4.1. Using these interpolating polynomials, we could keep the locations of the wells fixed while controlling the barrier height E_B^+. Once we had a potential, we would place the probability distribution in the upper well and then measure the probability that the particle is in the upper well with time and use this information to obtain the Kramers' rate, as shown in Figure 4.2.

This technique was used to calculate the Kramers' rate for multiple barrier height and potentials and it was found to be in excellent agreement with equation 4.10. The same technique can be used to obtain the Kramers' rate when the temperature is not held fixed. In this case, the Kramers' rate is sensitive to the boundary conditions imposed on the temperature and on the precise values of α and β as shown in Figure 4.3.

We therefore conclude that the Kramers' rate is dependent on the heat capacity and thermal diffusivity of the system.
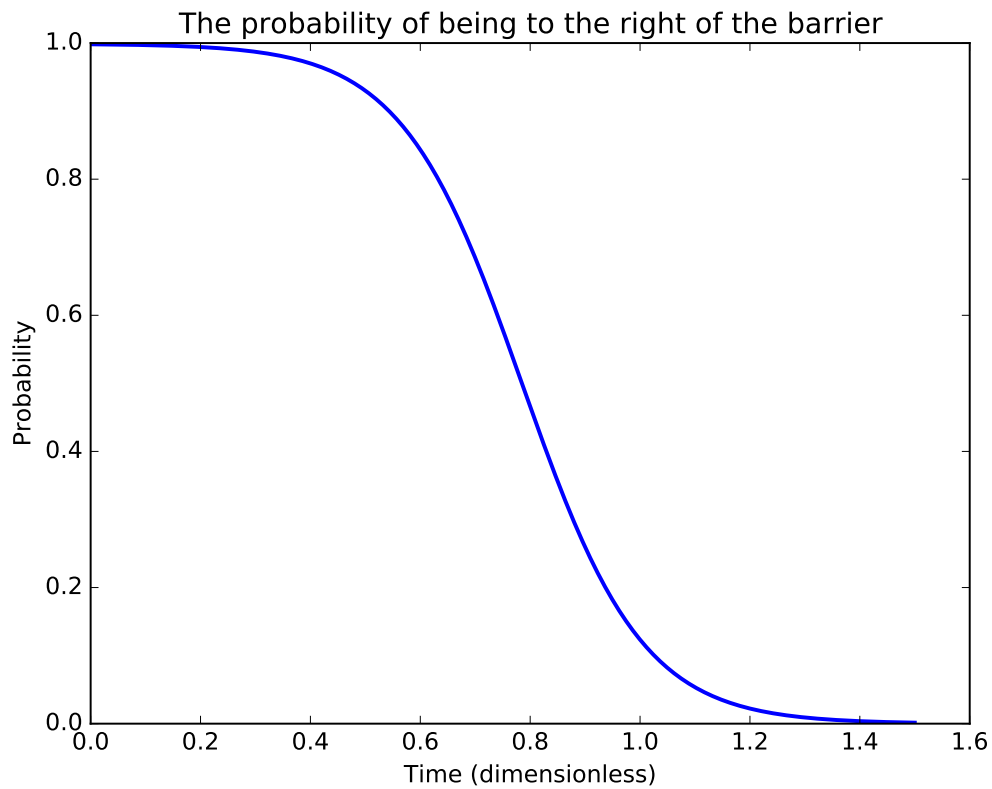
Figure 4.2: The probability of being to the right of the barrier. Here we see that the system decays into the ground state of the upper well and then begins to decay exponentially into the lower well. At the end of this, the probability of finding the particle on the upper well is almost zero. We can fit an exponential to this decay in order to estimate the Kramers' rate.
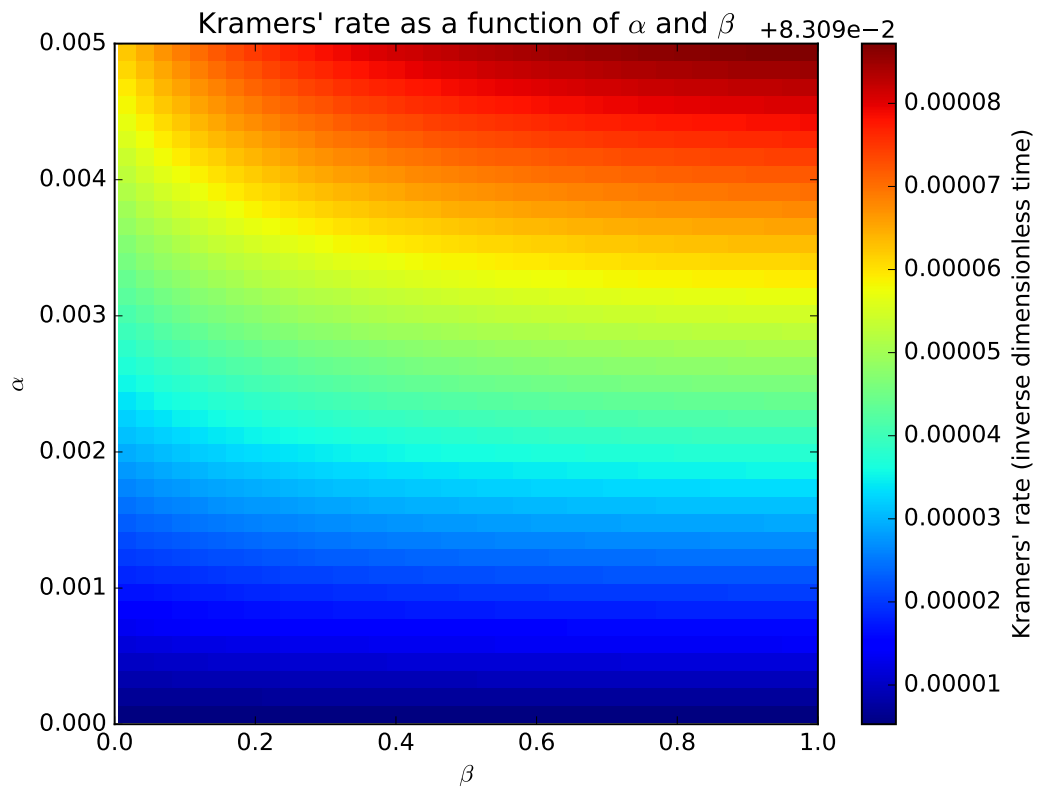
Figure 4.3: Kramers' rate Here we vary α and β and perform the same measurements as in Figure 4.2, the results show that the Kramers' rate varies with α and β.
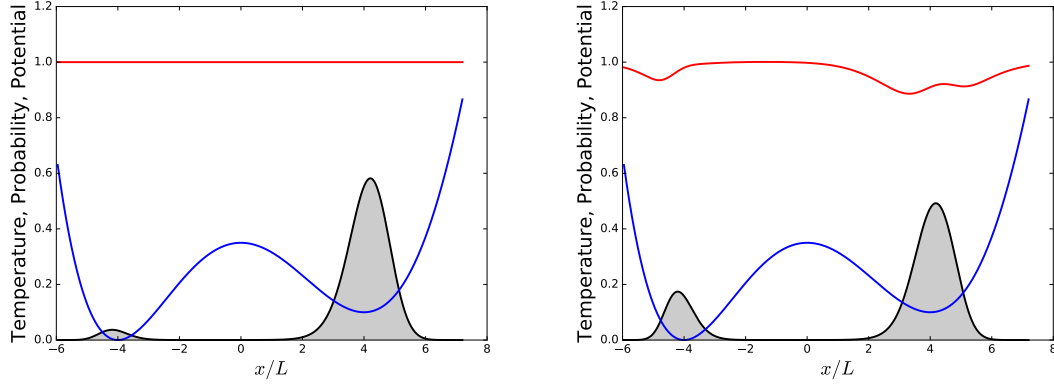
Figure 4.4: Reverse Landauer blowtorch effect. (a) The system starts off in the upper well of a bistable potential with a uniform temperature, we have $\alpha = 8 \cdot 10^{-2}$ and $\beta = 1.5$. (b) As the system decays into the lower well, the bath loses thermal energy in the form of heat, thus we see Brownian cooling as a consequence of the forcing of the potential. In these simulations Dirichlet boundary conditions were imposed, meaning that the temperature at the ends was held fixed. This means that there was heat flowing through the boundaries. This heat was calculated at each time step and used to update the energy at each time step. This is necessary because the numerics use the energy to normalize the temperature as mentioned in § 3.2.

## 4.1.2   The reverse Landauer blowtorch

As noted in   subsection 1.3.2, the relative occupancy of wells depends on the spatial distribution of the temperature, meaning that the temperature can act as a pseudo-force. However, it has been noted that when the movement of the particle has an effect on the environment, the opposite can occur [29]. Concretely, the the reverse Landauer blowtorch effect says that if there is a force applied to a Brownian particle, then the force will cause the particle to induce a temperature gradient in the environment. This is shown in Figure 4.4, in this figure, the temperature is held fixed at the boundaries, which we interpret physically as meaning that the domain is embedded in a much larger system that is held at a fixed temperature. Another example of a stochastic process that has an effect on the temperature of the environment is the Soret-Dufour effect, which has been observed experimentally [32–34]. In the Soret effect or the Dufour effect, a non-equilibrium concentration of molecules is capable of producing a temperature gradient. Ref [35] showed that thermal gradients due to the Soret effect have to be taken into account to explain measurements performed on protein crystal growth. Despite the knowledge of these self-induced temperature gradients, to our knowledge, Figure 4.4 is the first concrete demonstration of Brownian cooling as described by a self consistent theoretical model.

4.2   Titlted periodic potentials

Tilted periodic potentials are very important in biology where they can be used to model molecular motors. In Ref [48, 49] the authors synthesize a tilted periodic potential by placing Brownian particles on a crystalline surface. The surface is then titled at an angle θ relative to the normal defined by gravity, in their theoretical analysis, the authors assume a constant temperature and are therefore able to describe a non-equilibrium steady state. Interestingly, in § 3.1, we showed that our system does not have such a well defined steady state for tilted periodic potentials.

Despite not being able to easily calculate the steady state for titled periodic potentials, we can still explore the dynamical case as shown in Figure 4.5. In this figure, we have shown a potential with very shallow wells, physically this corresponds to a situation that is very far out of equilibrium. In this case, the self-induced temperature gradients have an effect on the shape of the probability density in the wells, but they do not change the flow down the potential very much. The tilted periodic potential combines the physics of both the Kramers' rate and the reverse Landauer blowtorch as described in § 4.1. One can imagine the potential in Figure 4.5 as being a multi-stable potential as opposed to the bistable potential shown in Figure 4.1. In fact, noticing that the titled periodic potential is a multi-stable potential led the authors of Ref [50] to describe a periodic potential with a master equation that involved the Kramers' rate of each of the adjacent wells. As well as the return of the Kramers' rate, Figure 4.5 is a very good demonstration of the reverse Landauer blowtorch effect. One can see from looking at the figure that the Brownian particle is absorbing heat from the environment as it moves down the potential. We therefore speculate that the reverse Landauer blowtorch effect could have an effect on biological molecular motors.

In order to quantify the effect of α and β on titled periodic wells we will turn to potentials that have deep wells. In these potentials the probability distribution will be very strongly localized at the bottom of the wells and will be hopping from well to well as explained in subsection 4.1.1. As the particle hops between wells, it will reduce the temperature in the well that it is currently situated in. If α is made large enough, then the Landauer blowtorch effect may cause the particle to hop back into the well that it came from. This is shown in Figures 4.6 and 4.7, here we see that there is a critical value of α. Below this critical value, the self-induced temperature gradient will not be substantial so the particle will hop out of the higher well and drift down the potential. If α is above the critical value, however, then the self-induced temperature gradient caused by the movement of the particle will cause the particle to actually move back into the well that it came from, at the same time causing the temperature of that well to decrease. Eventually the particle reaches a steady state where the temperature gradient causing the particle to move against the potential is exactly canceled by the force of the potential itself. When one is at the critical value of α, the probability distribution does not fully leak out of the initial well or hop back into it and instead will be constantly balancing between these two limits. This critical value is highly sensitive to α, the probability may remain flat for quite some time only to either hop down to the lower well or hop back up into the higher well. In the context of molecular motors, values of α greater
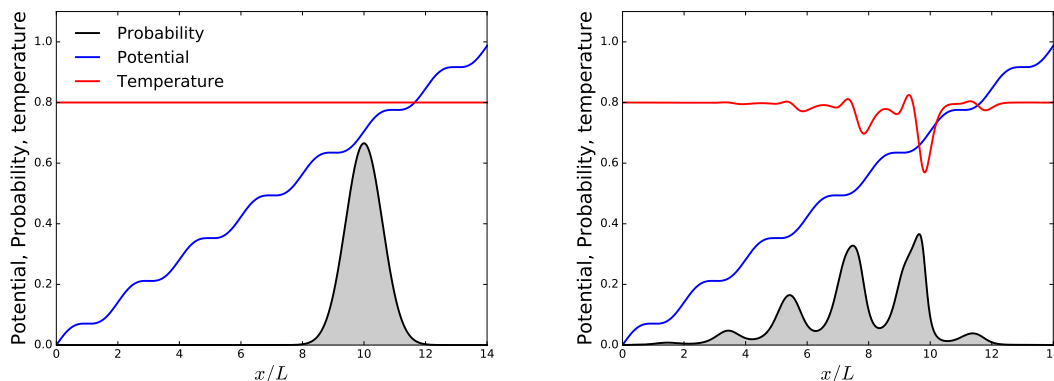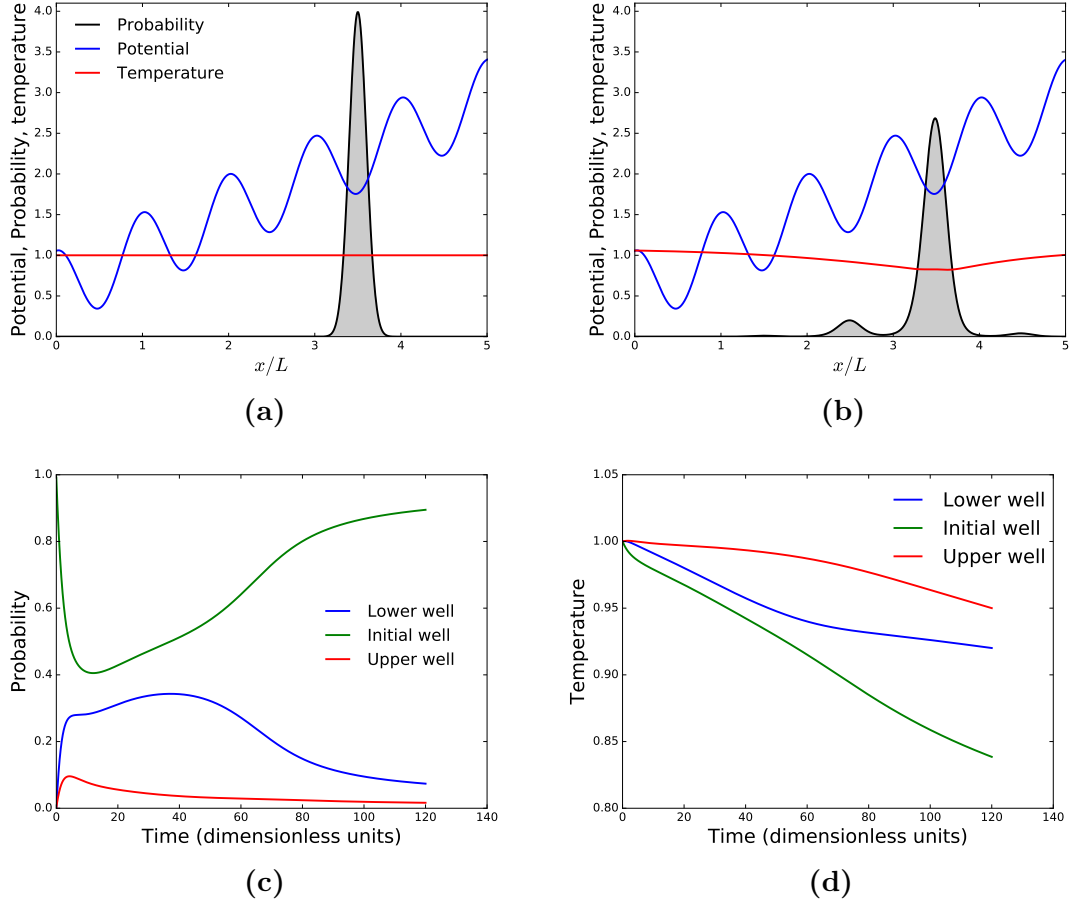
Figure 4.5: Tilted periodic potential with shallow wells. Imposing Dirichlet boundary conditions maintaining that the temperature is equal to 0.8 at the boundaries (temperature is dimensionless), we have $\alpha = 1 \cdot 10^{-4}$ and $\beta = 1 \cdot 10^{-2}$. (a) The system begins with a uniform temperature with a Gaussian probability distribution located near the top of the potential. (b) after some time, the particle has moved down the potential, removing heat from the environment as it overcomes the periodic barriers provided by the potential. We notice that unlike Figure 1.2, the probability distribution does not decay into Gaussian distributions in the wells, instead the temperature gradients cause the probability distribution to take on a very complicated form.

than the critical value would correspond to a stall.

Instead of changing the value of α in Figure 4.7, we could have changed the tilt of the potential. Both cases lead to the same unstable critical behavior. In Figure 4.7, we show the population for many different values of α. Here we see that if one explores values of α around the critical value, then as one goes forward in time, the trajectories of the probability distribution will bifurcate. If one then looks at the values of α near these bifurcations, then one will find that after some time another bifurcation occurs. This chaotic behavior is to be expected for non-linear equations and shows that the behavior of equations 2.6 and 2.7 can be highly sensitive to the properties of the environment. From these figures it appears that the particle is heading towards a bound state where the particle is localized almost entirely in the well that it started in. Since we were free to choose the initial configuration of the probability density, it would seem that the long term steady-state is not unique. This is not true, the particle is in fact converging on a quasi-steady state that it will eventually decay out of. To see this, note that if the particle has reached a truly steady state then the current $J(x, t)$ is zero, therefore equation 2.7 reads

$$\frac{\partial T(x, t)}{\partial t} = \frac{\partial^2 T(x, t)}{\partial x^2}, \tag{4.14}$$

the solution to this equation in the steady state is a straight line. In this case the evolution of the particle should be given by the Smoluchowski equation which is known to have no locally bound solutions.

(a)

(b)

(c)

(d)

Figure 4.6: Stalling in the tilted periodic potential $\alpha = 8.3 \times 10^{-5}$ and $\beta = 1 \times 10^{-2}$ (a) The initial configuration. We have a tilted periodic potential with deep wells and a constant temperature. (b) Even after a long time the probability density is not able to completely leak out of it's initial well, this is because the particle has cooled down the initial well therefore making this state more favorable due to the Landauer blowtorch effect. (c) Population of the wells, for clarity we have only included the initial well and the wells adjacent to it. The particle begins entirely located in the upper well and begins to leak into the adjacent wells, at about 15 dimensionless time units, the temperature of the initial well is so low that the particle actually moves against the potential gradient. (d) Temperature of the wells, we simply calculated the mean temperature of each well.

(a)   (b)

(c)
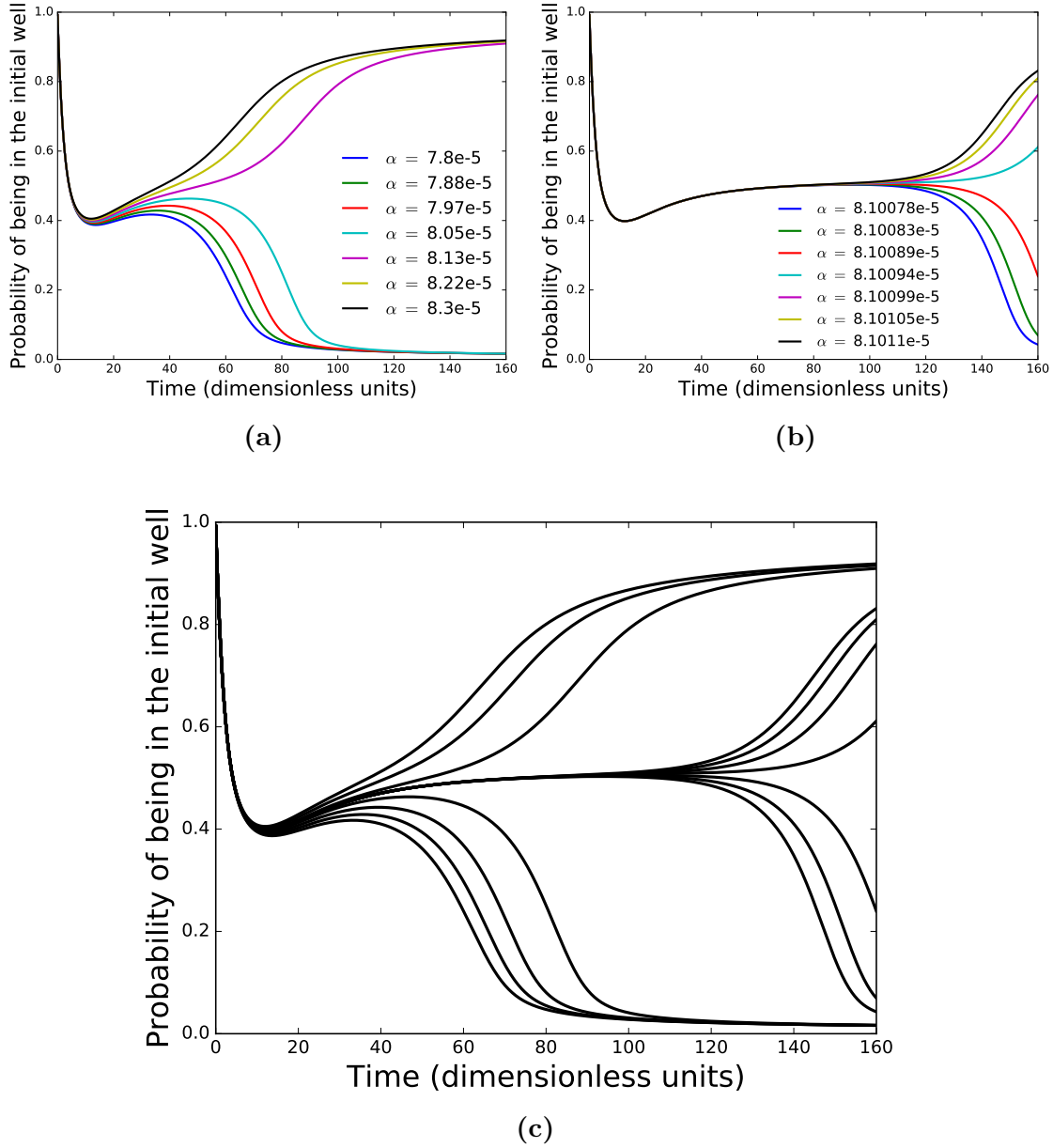
Figure 4.7: The population of the initial well for different values of α (a) We have a moderately large rage of values of α, when α is below the critical value, the probability density hops from the upper well into the lower one. If α is above the critical value, then initially it will leak into the lower well while simultaneously cooling the initial well, when the initial well becomes cold enough the particle will hop back into it's initial state due to the Landauer blowtorch effect. (b) Here we consider values of α either side of the critical value, in this case the probability distribution spends some time stuck between wells and then it bifurcates, this shows that the long term behavior of the probability distribution is extremely sensitive to α. (c) Here we have overlaid the lines from parts (a) and (b) to show the second bifurcation more explicitly, we speculate from this bifurcation that equations 2.6 and 2.7 may have fractal type behavior.

41

Chapter 5

Discussion

> I say that the physics works by pixies, you say that the physics works by gnomes.

<div align="right">

Associate Professor Colin Fox − 2016

</div>

Brownian dynamics is an area of research that is of interest from the perspective of basic physics as well as applied physics. In this thesis we have discussed Brownian dynamics from a very basic point of view and we have focused in particular on the role of self-induced temperature gradients in the equations of motion. We have created a self-consistent description of Brownian dynamics that fully describes the flow of energy and entropy through a system. The fact that our system has a well defined entropy is a strong advantage and allows one to talk about information in a rigorous way [41, 42]. Moving beyond the analytical solutions, we found that allowing self induced temperature gradients could have a very complicated effect on the evolution of a system. As the Brownian particle evolves in a potential it creates temperature gradients that effect the future diffusion of the particle, thus creating a rich interaction between the Brownian particle and it's environment. The dynamical behavior of the Brownian particle was fully described using numerical techniques, these numerical techniques were tested thoroughly using convergence tests and by a comparison to analytical solutions. Using our numerical techniques, we made concrete observations of the reverse Landauer blowtorch effect. We also saw that self-induced temperature gradients had an effect on the Kramers' rate and that they could cause a Brownian particle to go into a quasi-stable state where the particle becomes stuck in a particular well.

The equations that we have used are self consistent in that they describe a system that obeys the laws of thermodynamics. Despite this, we believe that due to assumptions made at the beginning of the thesis, the equations can only describe a limited number of systems actually realized in nature and in chapter 6 we will discuss how the system could be generalized to incorporate physical phenomena from disciplines outside of statistical mechanics. Despite the fact that our system does not describe a large number of situations in nature, the lessons learned from studying our system will be extremely useful in modeling different situations. In particular, by observing self induced temperature gradients through numerical simulations we have been able to make concrete observations of the reverse Landauer blowtorch as

well as the effect of thermal diffusivity and the specific heat of the environment on the Kramers' rate.

Purely from a theoretical stand-point, the inclusion of self-induced temperature gradients better explains the flow of energy and entropy through a system. In § 2.3 we explained how the temperature of the environment is a crucial player in the calculation of the entropy and energy of a system. In the case of deep wells, self-induced temperature gradients can actually cause the particle to stop moving with the force of the potential. This is an unexpected consequence of the reverse Landauer blowtorch and leads to some very interesting non-linear behavior. This is particularly interesting in Brownian motors, where the effect could lead to a stall in the motor, we speculate that biological systems will have mechanisms in place to avoid these stalls because a motor stall would mean that the motor would no longer be able to perform it's designated task.

Chapter 6

Outlook

Our work is valid under certain assumptions, future work could build on our work could build on our results by relaxing these assumptions, we summarize this below.

- Generalization to 2d and 3d systems

- Inter-particle interactions

- Flow of heat via convection as well as an extension to compressible fluids and gases

- Implications to information theory

6.1 Generalization to 2d and 3d systems

Many systems of interest are multi-dimensional and cannot be approximated by a one-dimensional system [1, 2, 13, 27, 50]. In particular, finding the efficiency of a molecular motor involves calculating the flow of energy from one degree of freedom to another [27]. Furthermore, generalizing our system to more dimensions gives more directions in which heat can flow, therefore allowing us to conserve energy in a more general sense. The equations motion in multiple dimensions can be written as:

$$\mathbf{J}(\mathbf{x},\,t) = -(P(\mathbf{x},\,t)\nabla V(x) + k_B T(\mathbf{x},\,t)\nabla P(\mathbf{x},t)) \tag{6.1}$$

$$\frac{\partial P(\mathbf{x},\,t)}{\partial t} = -\nabla \cdot \mathbf{J}(\mathbf{x},\,\mathbf{t}) \tag{6.2}$$

$$\frac{\partial T(\mathbf{x},\,t)}{\partial t} = -\kappa \mathbf{J}(\mathbf{x},\,\mathbf{t}) \cdot \nabla V(\mathbf{x},\,t) + D\nabla^2 T(\mathbf{x},\,t) \tag{6.3}$$

6.2 Inter-particle interactions

Inter-particle interactions play a very important role in Brownian dynaimcs [16, 17], an example of this is the myosin protein in cells which is used in the contraction of muscles [51]. Individually, myosin proteins are poor at carrying loads

when compared to their kinesin couterparts [51], however their collective actions are very powerful due to the rich nature of their inter-motor interactions.

The set of equations that we have been using do not apply to more than one Brownian particle without some considerable changes. This is due to very complicated inter-particle interactions that can occur when considering thermal fluctautions of the kind that we are focusing on. To visualize this intuitively, imagine two particles diffusing in their reaction coordinates, both subject to the same potential. Particle one may induce local temperature gradients that will affect particle two if particle two moves to where particle one created those temperature gradients. These interactions involve second-order statistics that are beyond the scope of this project.

6.3   Fluid dynamics

The Brownian particles that we have been modelling have been suspended in a fluid. The dynamics of fluids present a formidable and exciting challenge to both physicists and mathematicians alike. As well as this there has been effort in the literature to combine the Smoluchowski equation with the Navier-Stokes equation, thus linking the world of Brownian dynamics with fluid dynamics [52]. The two physical phenomena that we neglect which could be treated with techniques from fluid dynamics are compressible fluids and heat convection through fluid flow. Despite the fact that we neglected these phenomena, our system is still physical and is self-consistent.

In § 2.3, in order to gain insight on the entropy we had to assume that we were dealing with an incompressible fluid. Without this assumption, we would not be able to guarantee that our equations of motion increase the entropy. Therefore, in order to obey the laws of thermodynamics in a compressible fluid, we would have to include extra terms in our equations of motion.

The second important phenomena that can be described by fluid dynamics is fluid flow. This phenomenon is responsible for heat transport via convection, currently we only consider heat flow via diffusion, this means that we are tacitly assuming that the fluid in which our Brownian particle is suspended, is stationary. Including convection into our model would involve modifying the heat equation (equation 2.7) so that it reads

$$\frac{\partial T}{\partial t} + u(x)\frac{\partial T}{\partial x} = -\kappa J \partial_x V + D\frac{\partial^2 T}{\partial x^2} \tag{6.4}$$

Where $u(x)$ represents the flow of the fluid, one can imagine that such a flow would have an effect on the system by transporting the temperature gradients with the flow of the fluid. The next step in including fluid dynamics into the system would be to introduce the Navier-Stokes equations into our system, thus yielding three coupled equations to solve.

6.4 Information theory and computation with Brownian particles

The link between statistical mechanics and information theory has been established by Landauer [42]. In this paper Landauer considers bi-stable potentials similar to those discussed in § 4.1. He then uses statistical mechanics to show that the erasure of information is associated with a generation of entropy, this therefore puts a theoretical lower bound on the amount of heat that a computer must produce in order to operate. Ref [41] gives an experimental realization of information storage and retrieval using a levitating colloidal particle. Our model considers the flow of heat and its effect on the environment explicitly, therefore an obvious future project would be to reconsider Landauer's logic in the case of self-induced temperature gradients. By considering the effect that the Brownian particle has on the environment, one could possibly gain some considerable insight into the role of statistical mechanics in computation.

Bibliography

[1] David Keller and Carlos Bustamante. The Mechanochemistry of Molecular Motors. *Biophysical Journal*, 2000.

[2] Peter Reimann. Brownian Motors: noisy transport far from equilibrium. *Physics Reports*, 2001.

[3] R Dean Astumian. Design principles for Brownian molecular machines: how to swim in molasses and walk in a hurricane. *Physical Chemistry Chemical Physics*, 9(37):5067–5083, 2007.

[4] Robert Brown. A Brief Account of Microscopical Investigations on the Particles Contained in the Pollen of Plants. *Privately circulated in 1828*, 1828.

[5] A Einstein. On the movement of small particles suspended in stationary liquids required by the molecular-kinetic theory of heat. *Ann. Phys*, 17:549–560, 1905.

[6] Jean Perrin. *Brownian movement and molecular reality*. Courier Corporation, 2013.

[7] R. F. Streater. Non linear heat equations. *Reports on Mathematical Physics*, 1997.

[8] R. F. Streater. A Gas of Brownian Particles in Statistical Dynamics. *Journal of Statistical Physics*, 1997.

[9] R. F. Streater. The soret and dufour effects in statistical dynamics. *Proceedings of the Royal Society of London A: Mathematical, Physical and Engineering Sciences*, 456(1993):205–221, 2000.

[10] R. F. Streater. Dynamics of Brownian particles in a potential. *Journal of Mathematical Physics*, 38:4570–4575, September 1997.

[11] Crispin Gardiner. *Stochastic methods*. Springer, 2009.

[12] Rob Phillips and Stephen R. Quake. The Biological Frontier of Physics. *Physics Today*, May 2006.

[13] Marcelo O. Magnasco. Molecular combustion motors. *Physical Review Letters*, 1994.

[14] Phillip Nelson. *Biological Physics: Energy, Information, Life*. W.H. Freeman and Company, 2014.

[15] Anke Treuner-Lange Janet Iwasa Lotte Søgaard-Andersen Grant J. Jensen Yi-Wei Chang, Lee A. Rettberg. Architecture of the type IVa pilus machine. *Science*, 2016.

[16] S Leibler and D A Huse. Porters versus rowers: a unified stochastic model of motor proteins. *The Journal of Cell Biology*, 121(6):1357–1368, 1993.

[17] S Leibler and DA Huse. A physical model for motor proteins. *Comptes rendus de l'Academie des sciences. Serie III, Sciences de la vie*, 313(1):27–35, 1990.

[18] Valentin Blickle and Clemens Bechinger. Realization of a micrometre-sized stochastic heat engine. *Nature Physics*, 2011.

[19] Pedro A. Quinto-Su. A microscopic steam engine implemented in an optical tweezer. *Nature Communications*, 2014.

[20] Steven A. Henck Michael W. Deem Gregory A. McDermott James M. Bustillo John W. Simpson Gregory T. Mulhern Joel S. Bader, Richard W. Hammond and Jonathan M. Rothberg. Dna transport by a micromachined Brownian ratchet device. *PNAS*, 1999.

[21] Zhisong Wang. Bio-inspired track-walking molecular motors (perspective). *Biointerphases*, 5(3):FA63–FA68, 2010.

[22] Max von Delius, Edzard M Geertsema, and David A Leigh. A synthetic small molecule that can walk down a track. *Nature chemistry*, 2(2):96–101, 2010.

[23] Max von Delius, Edzard M Geertsema, David A Leigh, and Dan-Tam D Tang. Design, synthesis, and operation of small molecules that walk along tracks. *Journal of the American Chemical Society*, 132(45):16134–16145, 2010.

[24] Richard Feynman. *Feynman lectures on physics*. California Institute of Technology, 1963.

[25] Rolf Landauer. Motion out of noisy states. *Journal of Statistical Physics*, 53(1):233–248, 1988.

[26] Juan M. R. Parrondo and Pep Español. Criticism of Feynman's analysis of the ratchet as an engine. *American Journal of Physics*, 64(9):1125–1130, 1996.

[27] C. Tumlin M. W. Jack. Intrinsic irreversibility limits the efficiency of multi-dimensional brownian motors. *Physical Review E*, 2016.

[28] NG van Kampen. Explicit calculation of a model for diffusion in nonconstant temperature. *Journal of mathematical physics*, 29(5):1220–1224, 1988.

[29] Moupriya Das, Debojyoti Das, Debashis Barik, and Deb Shankar Ray. Landauer's blowtorch effect as a thermodynamic cross process: Brownian cooling. *Phys. Rev. E*, 92:052102, Nov 2015.

[30] Schnapp BJ. Block SM, Goldstein LS. Bead movement by single kinesin molecules studied with optical tweezers. *Nature*, 1990.

[31] Hendrik Anthony Kramers. Brownian motion in a field of force and the diffusion model of chemical reactions. *Physica*, 7(4):284–304, 1940.

[32] Lars Onsager. Reciprocal relations in irreversible processes. i. *Phys. Rev.*, 37:405–426, Feb 1931.

[33] W. Hort, S. J. Linz, and M. Lücke. Onset of convection in binary gas mixtures: Role of the dufour effect. *Phys. Rev. A*, 45:3737–3748, Mar 1992.

[34] Roberto Piazza and Andrea Guarino. Soret effect in interacting micellar solutions. *Phys. Rev. Lett.*, 88:208302, May 2002.

[35] I Santamaría-Holek, A Gadomski, and J M Rubí. Controlling protein crystal growth rate by means of temperature. *Journal of Physics: Condensed Matter*, 23(23):235101, 2011.

[36] Edward T Jaynes. Gibbs vs boltzmann entropies. *American Journal of Physics*, 33(5):391–398, 1965.

[37] Yunus A Cengel and Michael A Boles. Thermodynamics: an engineering approach. *Sea*, 1000:8862, 1994.

[38] J. Crank and P. Nicolson. A practical method for numerical evaluation of solutions of partial differential equations of the heat-conduction type. *Advances in Computational Mathematics*, 6(1):207–226, 1996.

[39] William H Press. *Numerical recipes 3rd edition: The art of scientific computing*. Cambridge university press, 2007.

[40] Jeff Bezanson, Alan Edelman, Stefan Karpinski, and Viral B. Shah. Julia: A Fresh Approach to Numerical Computing. *CoRR*, abs/1411.1607, 2014.

[41] Christopher J Myers, Michele Celebrano, and Madhavi Krishnan. Information storage and retrieval in a single levitating colloidal particle. *Nature nanotechnology*, 10(10):886–891, 2015.

[42] Rolf Landauer. Irreversibility and heat generation in the computing process. *IBM journal of research and development*, 5(3):183–191, 1961.

[43] Joseph D Bryngelson and Peter G Wolynes. Intermediates and barrier crossing in a random energy model (with applications to protein folding). *The Journal of Physical Chemistry*, 93(19):6902–6915, 1989.

[44] Bruce J Berne and Robert Pecora. *Dynamic light scattering: with applications to chemistry, biology, and physics*. Courier Corporation, 1976.

[45] Victor Barcilon. Eigenvalues of the one-dimensional Smoluchowski equation. *Journal of Statistical Physics*, 82(1):267–296, 1996.

[46] I Santamaría-Holek, A Gadomski, and J M Rubí. Controlling protein crystal growth rate by means of temperature. *Journal of Physics: Condensed Matter*, 23(23):235101, 2011.

[47] Henry Eyring. The activated complex in chemical reactions. *The Journal of Chemical Physics*, 3(2):107–115, 1935.

[48] Xiao-guang Ma, Pik-Yin Lai, Bruce J Ackerson, and Penger Tong. Colloidal transport and diffusion over a tilted periodic potential: dynamics of individual particles. *Soft matter*, 11(6):1182–1196, 2015.

[49] Xiao-guang Ma, Pik-Yin Lai, Bruce J Ackerson, and Penger Tong. Colloidal dynamics over a tilted periodic potential: Nonequilibrium steady-state distributions. *Physical Review E*, 91(4):042306, 2015.

[50] Katharine J Challis and Michael W Jack. Energy Transfer in a Molecular Motor in Kramers' Regime. *Biophysical Journal*, 106(2):371a–372a, 2014.

[51] Matthew J Tyska and David M Warshaw. The myosin power stroke. *Cell motility and the cytoskeleton*, 51(1):1–15, 2002.

[52] Peter Constantin. Smoluchowski Navier-Stokes systems. *Contemporary Mathematics*, 429:85, 2007.

Appendices

Appendix A

Additional figures

I am a fish.

Dr. Philip Brydon – 2016

There are a lot of interesting phenomena that occur when one explores the system that we explored in detail. In this appendix, we would like to share some of the exciting results that we found during the project, these results do not directly contribute to the narrative of the thesis which is why they were not included in the main body of the text. Despite not being a part of the main body, we feel that the reader would be at a loss without being made aware of these phenomena.